UNIVERSITY OF KWA-ZULU NATAL

SIGNAL SPACE DIVERSITY WITH AND WITHOUT ALAMOUTI TRANSMIT DIVERSITY USING GENERALISED SELECTION COMBINING

Aadil Essop

Supervised by: Prof Hongjun Xu

Submitted in fulfilment of the degree of Master of Engineering,
School of Engineering, University of Kwa-Zulu Natal, Durban, South Africa
Jan 2015

As the supervisor of this student, I hereby agree to the submission of his dissertation.

Date of Submission: _____

Supervisor: _____

Professor H. Xu

Declaration 1

I, Aadil Essop, declare that,

i) This research has not been previously accepted for any degree and is not being currently considered for any other degree at any other university.

ii) The work contained in this dissertation is my own work, except when otherwise stated.

iii) This dissertation contains original pictures, graphs or other sources of information unless specifically mentioned and acknowledged as being part of another person/s work.

iv) This dissertation does not contain other person/s writing unless specifically mentioned as referenced accordingly.

v) All publications have clearly outlined my contribution and contain references for any other sourcing of information.

vi) All tables, figures and graphs have been originally produced and have not been copied from other sources, unless otherwise stated and acknowledged accordingly.

Signed: _____

AADIL ESSOP

January 2014

Declaration 2

DETAILS OF CONTRIBUTION TO PUBLICATIONS that form part and/or include research presented in this dissertation (include publications in preparation, submitted, *in press* and published and give details of the contributions of each author to the experimental work and writing of each publication)

Submission 1:

A. Essop and H. Xu, "Symbol Error Rate of Generalized Selection Combining with Signal Space Diversity in Rayleigh Fading Channels,"2014

Submitted to SAIEE - Africa research journal

Submission 2:

A. Essop and H. Xu, "Alamouti Space-Time Coded M-QAM with Signal Space Diversity and Generalized Selection Combing in Rayleigh Fading Channels," Symbol Error Rate of Generalized Selection Combining with Signal Space Diversity in Rayleigh Fading Channels", 2014

Prepared for submission.

Acknowledgements

I would like to thank God for his blessings and assistance in helping me achieve my goals.

I would then like to thank my supervisor, Professor Hongjun Xu, for the motivation and guidance which helped me complete this dissertation. He has thought me many skills that successfully helped me perform research. His dedication and perseverance is an inspiration. I would then like to thank the centre of excellence, UKZN, for financially supporting me during this endeavour.

I would like to thank my family, who would often work around my schedule to accommodate me as I would often be busy with my research. They provided me with a cosy environment and motivated me into performing at my best. Lastly I would like to thank my friends who would often provide me with words of encouragement and advice.

Abstract

The first contribution is based on M-ary quadrature amplitude modulation (M-QAM) constellations with signal space diversity (SSD) using a single transmit and L receive antenna system in the presence of Rayleigh fading. Two commonly used techniques to derive an angle of rotation is investigated across different ordered M-QAM signal constellations to determine the optimum angle of rotation for this system. Thereafter a closed form expression using the nearest neighbour (NN) approach to quantify the symbol error rate (SER) in the presence of fading channels is presented. The diversity order and the signal-to- noise ratio (SNR) gap is investigated for different generalised selection combining (GSC) cases for an M-QAM with SSD system.

The second contribution is based on an Alamouti coded M-QAM scheme with SSD and GSC using a two transmit and L receive antenna system in the presence of Rayleigh fading. A closed form expression using the NN approach is used to accurately derive the SER performance of an Alamouti coded M-QAM with single rotated SSD and GSC system. An additional level of diversity is added by rotating a constellation once again. Simulation results of M-QAM with double rotated SSD and GSC are used to compare the actual performance differences between single and double rotated SSD for this system. All deductions presented are validated with the aid of simulations.

Table of Contents

List of Figures

List of tables

List of acronyms

3G	3rd Generation
4G	4th Generation
AWGN	Additive White Gaussian Noise
BER	Bit Error Rate
CSI	Channel State Information
DVB-NGH	Digital terrestrial Video Next Generation Handheld
DVB-T2	Digital terrestrial Video Broadcasting system
FER	Frame Error Rate
GSC	Generalised Selection Combining
GSM	Global System for Mobile communications
i.i.d	Independent and Identically Distributed
LTE	Long Term Evolution
MED	Minimum Euclidean Distance
MGF	Moment Generating Function
MIMO	Multiple Input –Multiple Output
MISO	Multiple Input –Single Output
ML	Maximum likelihood
MPD	Minimum Product Distance
M-QAM	M-ary Quadrature Amplitude Modulation
MRC	Maximum Ratio Combining
MSLB	Multiple Sphere Lower Bound
MSUB	Multiple Sphere Upper Bound
NN	Nearest Neighbour
PDF	Probability Density Function
PEP	Pairwise Error Probability
SC	Selection Combing
SER	Symbol Error Rate
SNR	Signal-to-Noise Ratio
SSD	Signal Space Diversity.
STBC	Space Time Block Codes

Part I

Introduction

1. Introduction

Technology has revolutionised the way in which the world is now connected with wireless connectivity becoming more prominent in recent devices. In the last decade wireless communication usage increased at an exponential rate leading to bottle necking of data throughput, increased interference and other communication shortfalls in terms of reliability and speed.

Previously wireless communications were primarily required for less intensive, low bandwidth consumption such as voice calls and text messaging. Today wireless communication is employed for video streaming/calling, broadband internet and even gaming, all of which requires high bandwidth and a low latency connection. This creates an increased requirement for enhanced, faster, more steadfast wireless communication systems.

There have been many advances in different wireless communication techniques which are applied in communications today. Previously the global system for mobile communications (GSM) was the primary underlying communications infrastructure which provided low bandwidth connectivity for basic mobile cell-phone activity. Today, we have fourth generation (4G) mobile networks, such as the long term evolution (LTE) and LTE advanced networks [1] which offer high speed connectivity. New advances in mobile wireless communications strive for minimising power consumption and size whilst having an overall net improvement on communications. However, just as GSM became inadequate to connect the world, these new advances in LTE networks will soon be incapable of keeping the world connected too. This drives a constant demand for further advances in communications and motivates one into investigating alternative means to improve communications.

Reducing the effects of multipath fading will result in communication improvements as multipath fading contributes considerably to performance reductions in wireless networks [2]. Diversity techniques have been applied to combat the effect of fading and increase transmission link reliability. One of the most popular diversity techniques which has been investigated and applied in electronic devices is the use of multiple signal paths via the introduction of spatial diversity. Spatial diversity has been at the forefront of diversity techniques for many years and has been investigated and applied to mitigate fading. Recent electronic devices take advantage of spatial diversity techniques such as in the Samsung Galaxy S5, where multiple antennas are evident [3]. Mobile receiver nodes have the drawback of size and power constraints being imposed upon them, allowing only a certain number of antennas on the device. This fuels the demand for alternative diversity techniques which balance power, complexity and physical receiver size.

A simple transmit diversity technique more commonly known as Alamouti space time block coding (STBC) was proposed in [4] to introduce diversity into a system. It is one of the most commonly

applied space time block codes [5]. Alamouti makes use of transmit antenna diversity and time diversity in order to increase the overall diversity of a system.

Another example of a diversity technique that offers performance improvements is known as signal space diversity (SSD). SSD introduces diversity into a system without the cost of additional bandwidth or antennas [6], hence making it a suitable diversity technique for mobile communication enhancements.

The three main diversity techniques which are considered in this dissertation are spatial diversity with the use of generalised selection combining (GSC), SSD and Alamouti coding scheme. More details of these schemes will now be presented.

1.1 Spatial diversity – Generalized Selection Combining (GSC)

A typical signal travelling between two points which are not in line of sight, will in most cases experience what is known as multipath fading. This refers to the multiple paths a signal may follow during each transmission. Reflections, refractions, phase shifts, attenuations as well as interference all contribute to multipath fading. Spatial diversity is a diversity technique used to reduce the effects of multipath fading.

Multiple receive and/or transmit antennas provide multiple signal paths and the probability of all channels experiencing a deep fade at the same time is low, therefore providing diversity. Multiple channel systems use this as a means to improve bit error rate (BER) and/or symbol error rate (SER) performance [7]. Multiple – input multiple – output (MIMO), multiple – input single – output (MISO) and single – input multiple – output (SIMO) are systems which apply spatial diversity. The SER and/or BER performance can be improved by combining signals from multiple channels [8].

Two commonly used signal combing techniques are Maximum ratio combining (MRC) and selection combining (SC). MRC involves the combination of all receive antennas and hence results in optimal performance but at the cost of increased detection complexity due to combining signals from multiple antennas whilst SC selects a single branch based on the highest instantaneous signal-to-noise ratio (SNR) [9]. The complexity of combining signals with MRC is relatively high and becomes even more complex when applied to high complexity communication networks of today, such as when applying MRC to the popular third generation (3G) communication technique, wide band code division multiple access (WCDMA). On the other extremity SC, does not fully exploit all available receiver diversity [7]. In order to balance performance and complexity a hybrid scheme can be applied known as generalized selection combining (GSC) [7, 10].

Let L be the total available receiver antennas. In GSC a subset L denoted as L_C antennas are chosen from the highest SNR. GSC has the following terminology and is typically expressed as GSC (L_C, L).

Suppose that there are L independent and identically distributed (i.i.d.) fading channels. Let h_l be the fading coefficient and $\gamma_l = \frac{E_s}{N_0} |h_l|^2$ be the instantaneous SNR of each l^{th} diversity branch where $l \in [1:L]$ and $\frac{E_s}{N_0}$ is the SNR per symbol. Then the combined SNR using GSC can be written as [10].

$$\gamma_{GSC} = \sum_{l=1}^{L_c} \gamma_l \tag{1}$$

GSC can result in SC or MRC depending on the value of L_c. Due to the complexity drawback of MRC, GSC appeals as a more efficient solution to combat fading.

1.2 Signal space diversity (SSD)

The idea of rotating a signal constellation was first proposed in [11]. Rotated constellations form the basis of SSD which involves rotating a signal constellation about a certain angle. The rotation of a signal constellation is important in SSD, but the diversity which is gained can only be realised after the signal points have been component interleaved. These two operations exploit the inherent diversity of signal constellations.

A conventional M-ary quadrature amplitude modulation (M-QAM) signal constellation is rotated by a certain angle. Constellation rotations makes the system more immune to deep fading as no two points will collapse at the same time as stated in [6]. This is illustrated in the Fig.1 below and can be seen that if fading does occur, unlike the non-rotated constellation, the rotated constellation's four points each have different in – phase (real) and quadrature – phase (imag) components.

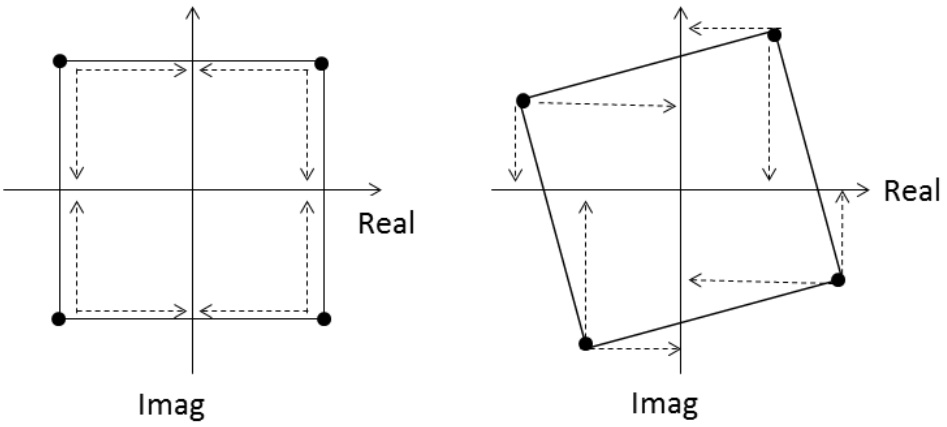

Fig. 1 : SSD diagram for 4-QAM [6]

Each constellation is rotated by a certain angle. The purpose of rotating is to achieve the maximum number of distinct components in the new rotated signal constellation [6], as this will ensure maximum performance in terms of SER. Two dimensional SSD has a maximum attainable diversity order of two [6]. In order to achieve diversity, is it assumed that no fading correlation between the in-

phase and quadrature components occur and this is achieved through the addition of component interleaving and de-interleaving before and after transmission respectively [12].

One of the benefits of exploiting SSD is that it does not require any additional bandwidth, transmission power or antennas. It does however require a more complex maximum Likelihood (ML) detector at the receiver. In [6], it was shown that the performance of a rotated constellation in a fading channel can perform as good as a non-rotated constellation in a pure additive white Gaussian noise (AWGN) channel. This shows that SSD focuses on combating the effects of fading. SSD results in a diversity order of two for 16-QAM [6]. Due to the many advantages of employing SSD, it has made its way into current communication standards which are being used today such as in the digital terrestrial video broadcasting system (DVB-T2) [13]. Conventional DVB-T2 applies a single rotation to achieve a maximum attainable diversity order of two with SSD. Further rotations have been applied in [14] to further increase the diversity of SSD. There is no limit on how many rotations one can have in SSD, but with each rotation an additional level of interleaving is required and hence a more complex detector will need to be used at the receiver. However, the BER/SER performance improvements will not be significant. According to [14], a new attainable diversity of four is achieved with the addition of a second rotation and interleaving/de-interleaving process. This was applied to increase the performance of digital terrestrial video next generation handheld (DVB-NGH). However, current literature does not present any analytical solution for double rotated constellations.

Rotational matrixes are applied to rotate the signal constellation. In [15], a complex matrix was applied whilst the most common matrix type still remaining the real matrix as can be viewed in [16, 17]. For the purpose of this dissertation a real rotational matrix will be applied for all constellation rotations given by [16].

$$\boldsymbol{R}^{\theta} = \begin{bmatrix} cos\theta & sin\theta \\ -sin\theta & cos\theta \end{bmatrix} \tag{2}$$

where θ is the rotational angle.

Different optimal angles have been applied depending on the system model. In **[**18**]**, two methods were considered for rotation angle. The design criterion as defined in **[**18**]** which is based on maximising the minimum Euclidean distance (MED) is a popular technique used to derive an optimal angle [18, 19]. The maximising of the minimum product distance (MPD) approach is an alternative criterion used to evaluate an optimal angle of rotation [18, 20].

SSD performance has been evaluated using various methods. Two of the most common evaluation methods which have been applied are the union bound and the nearest neighbour (NN) approximation. The union bound was applied in [6, 17, 20 - 23] whilst the NN approach was applied in [5, 16, 24].

Alternative performance evaluation techniques include the recently applied multiple sphere lower bound (MSLB) and multiple sphere upper bound (MSUB) approximations [25,26].

This dissertation applies SSD to an M-QAM constellation as a method to improve diversity.

1.3 Alamouti coding scheme

The Alamouti coding scheme was first presented in [4], as a means to introduce transmit and time diversity for wireless communications. The scheme consists of two transmit antennas and one receiver. This is a typical MISO system which utilises two channels for transmit antenna diversity. Furthermore a coding scheme proposed by Alamouti in [4], encodes the symbols to further improve performance of the system. The conventional Alamouti scheme is as follows.

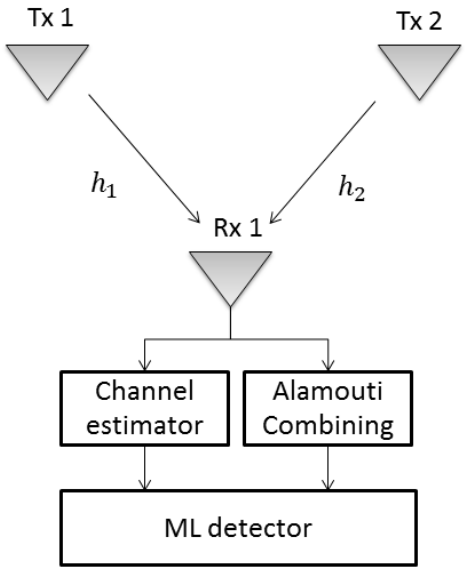

Fig. 2: Alamouti coding scheme

It is assumed that during each pair of time slots the fading remains constant with full channel state information (CSI) available at the receiver. Suppose two symbols will be transmitted s_1 and s_2 where both symbols are elements of a M-QAM signal constellation set with $E(|s_1|^2) = E(|s_1|^2) = 1$. Transmitting these symbols using Alamouti coding results in the follows during time slot T and $T + t$. The Alamouti combining scheme which is presented in [4] is applied before a conventional ML detector is used to estimate the symbols. Details of the transmit sequence can be viewed in Table 1.

Table 1 : Alamouti transmit sequence

Time	**TX 1**	**TX 2**
T	s_1	s_2
$T+t$	$-s_2^*$	s_1^*

where $(\cdot)^*$ represents the complex conjugate operator.

Alamouti provides an extremely useful method to improve SER/BER performance as it achieves double the receive antenna diversity without the addition of any receive antennas [4]. Similar to SSD, an Alamouti coding scheme requires the addition of an ML detector at the receiver, which brings one to recognise that combining an Alamouti coding scheme to SSD will result in both using the same ML detector and therefore not increase physical hardware requirements.

Performance evaluation of Alamouti coding is fairly simple to evaluate as it is mathematically equivalent to a single transmit antenna system with two receive antennas and half the transmit power [4]. This approach can be extended to an Alamouti coded M-QAM system with MRC to be mathematically equivalent to an MRC system with $2L$ receive antennas where L is the available receive antennas using half the transmit power.

2. Motivation and Research Objective

In [16, 17], M-QAM with SSD and MRC was presented and evaluated using the NN approach. However, [16] did not provide a closed form solution, but this was remedied in [17], where the union bound and NN was investigated and presented a closed form solution for M-QAM with SSD and MRC. Alamouti coded hierarchal modulated QAM with SSD was presented in [5]. As previously mentioned MRC has the drawbacks of high complexity, therefore motivating a suboptimal combining scheme choice known as GSC. M-QAM with SSD and GSC has not been presented in current literature. This motivates an investigation of an analytical closed form SER expression for M-QAM SSD using GSC.

Optimal angles of rotation have been researched in [17, 18, 20], different angles were considered dependent on the SSD system. In [18], the frame error rate (FER) for signal space cooperative communication was compared for two angles derived from the MED and MPD approach. Current research presents the importance of each criterion. However a direct comparison for the SER of M-QAM with SSD and GSC reception has not been presented for the different optimal angles. A direct comparison between the two primary techniques to derive an optimal angle will be presented.

The advantages of combining Alamouti STBC with other diversity techniques is significant and hence it has already been applied with SSD in [27] and this approach was extended for hierarchal modulated M-QAM with SSD in [5]. To the authors' best knowledge the SER of Alamouti coded M-QAM with SSD and GSC has not been investigated, revealing an avenue yet to be discovered. A closed form solution for an Alamouti coded M-QAM with SSD with GSC will be presented.

SSD with two rotations has been previously researched in [14] but this has not been investigated with Alamouti coded M-QAM or with GSC at the receiver. This motivates one to apply a second rotation and interleaving process on an Alamouti coded M-QAM with SSD and GSC system. The SER

improvements as well as the difference between a single and double rotated SSD in an Alamouti coded system will be presented.

3. Contributions of included papers

All research has been covered in detail in two papers which are presented in Part II. The details of the papers are as follows:

3.1 Paper A

A. Essop and H. Xu, "Symbol Error Rate of Generalized Selection Combining with Signal Space Diversity in Rayleigh Fading Channels,"2014

In paper A, M-QAM with SSD and GSC reception is presented. The NN approach is implemented and used to evaluate a closed form expression for the SER of M-QAM with SSD and GSC reception. The SER for different optimal rotation angles is also presented. The diversity gain of SSD with GSC is analysed for GSC and found to be related to the total number of receive antennas. The SNR gap power relationship between SC and MRC and hence GSC is also analysed, giving one a visual representation of the physical performance that is realised when using GSC and changing from SC to MRC. All findings presented are confirmed via simulations and can be viewed in paper A.

3.2 Paper B

A. Essop and H. Xu, "Alamouti Space-Time Coded M-QAM with Signal Space Diversity and Generalized Selection Combing in Rayleigh Fading Channels," Symbol Error Rate of Generalized Selection Combining with Signal Space Diversity in Rayleigh Fading Channels", 2014

In paper B, Alamouti M-QAM with SSD with GSC is investigated. Making use of the approach in paper A, paper B will expand this approach to include the SER of Alamouti coded M-QAM with SSD and GSC. A closed form expression for the SER is presented. The MGF for the fading coefficient of Rayleigh fading is used to evaluate the closed form SER solution. The use of a second rotation on an Alamouti coded M-QAM with SSD and GSC is investigated. The simulated performance is compared directly to an Alamouti M-QAM with SSD and GSC system. The simulation results is analysed and a conclusion is drawn from it.

4. Future Work

The first paper presents the SER performance of an M-QAM system with SSD and GSC reception whilst in the second paper, the SER performance of Alamouti coded M-QAM with SSD and GSC is investigated.

Both papers can be adapted to include a GSC switching algorithm which alters the value of L_C depending on the current SNR level. This is an interesting addition to the systems. The application of double rotated SSD has been discussed in previous literature, but to date no analytical solution has been presented, providing a further avenue of research.

5. References

[1] S. C. Chin, "LTE- Advanced technologies on current LTE service to overcome real network problems and to increase data capacity," in *IEEE ICACT*, PyeongChang, Jan 2013, pp. 275-281.

[2] A. Goldsmith, *Wireless Communications*. Cambridge: Cambridge Univ. press, 2005.

[3] A. J. Shepherd. (2014, March) S4GRU. [Online]. http://s4gru.com/index.php?/blog/1/entry-363-teaser-samsung-galaxy-s5-gets-a-boost-via-wi-fi-but-not-carrier-aggregation/

[4] S. Alamouti, "A simple transmit diversity technique for wireless communications," *IEEE, Selected areas on Commun.*, vol. 16, no. 8, pp. 1451-1458, Oct 1998.

[5] A. Saeed, H. Xu, and T. Quazi, "Alamouti space-time block coded hierarchical modulation with signal space diversity and MRC reception in Nakagami-m fading channels," *IET Commun.*, vol. 8, no. 4, pp. 516-524, Oct 2014.

[6] J. Boutros and E. Vitebro, "Signal Space Diversity: A Power-and Bandwidth- Efficient Diversity Technique," *IEEE Trans. on Info. Theory*, vol. 44, no. 4, pp. 1453 - 1467, July 1998.

[7] M. S. Alouini and M. K. Simon, *Digital Communications over Fading Channels: A Unified Approach to Performance Analysis*: A Wiley- Interscience Publication, 2000.

[8] K. Xu, "Antennas Selection for MIMO Systems over Rayleigh Fading Channels," in *ICCCAS*, Chengdu, 2004, pp. 185-189.

[9] A. I. Sulyman and M. Kousa, "Bit error rate performance of a generalized diversity selection combining scheme in Nakagami fading channels," in *IEEE Conf. Wireless Commun. and networking.* , Chicago, 2000, pp. 1080-1085.

[10] H. Xu, "Symbol Error Probability for Generalized Selection Combining," *SAIEE Research Journal*, vol. 100, no. 3, pp. 68-71, Sept 2009.

[11] J. Boutros, E. Viterbo, and C. Rastello, "Good lattice constellations for Both Rayleigh Fading and Gaussian Channels," *IEEE Trans. on Info. Theory*, vol. 42, no. 2, pp. 502-518, March 1996.

[12] A. Chindapol, "Bit-interleaved coded modulation with signal space diversity in Rayleigh fading," in *Signals, Systems and Computers Conf.*, Pacific Grove, CA, 1999, pp. 1003-1007.

[13] L. Polak and T. Kratochvil, "Comparison of the non-rotated and rotated constellations used in DVB-T2 standard ," in *Radioelektronika International*, Brno, 2012, pp. 1-4.

[14] J. Kim, H. Kim, T. Jung, J. Bae, and L. Gwangsoon, "New Constellation- Rotation Diversity Scheme for DVB-NGH," in *IEEE Trans. Veh. Technol.*, Ottawa, 2010, pp. 1-4.

[15] A. Correia, A. Hottinen, and R. Wichman, "Optimised constellations for transmitter diversity ," in *IEEE Trans. Veh. Technol*, Amsterdam , 1999, pp. 1785-1789.

[16] S. Jeon, I. Kyung, and M. K. Kim, "Component- Interleaved receive MRC with Rotated Constellation for Signal Space Diversity.," in *IEEE Conf. Veh. Technol*, Alaska, 2009, pp. 1-6.

[17] Z. Paruk and H. Xu, "Performance Analysis and Simplified Detection for Two - Dimensional Signal Space Diversity with MRC reception," *SAIEE Africa Research Journal*, vol. 104, no. 3, pp. 97-106, September 2013.

[18] S. A. Ahmadzadeh, "Signal space cooperative communication," *IEEE Trans. on wireless Commun.*, vol. 6, no. 4, pp. 1266-1271, April 2010.

[19] A. Saeed, T. Quazi, and H. Xu, "Hierarchical modulated quadrature amplitude modulation with signal space diversity and maximal ratio combining reception in Nakagami-m fading channels," *IET Commun.*, vol. 7, no. 12, pp. 1296-1303, Aug 2013.

[20] E. Viterbo and G. Taricco, "Performance of component interleaved signal sets for fading channels," *Electronic letters*, vol. 32, no. 13, pp. 1170-1172, April 1996.

[21] N. H. Tran, H. H. Nguyen and T. Le-Ngoc, "BICM-ID with Signal Space Diversity for Keyhole Nakagami-m Fading Channels," in *Info. Theory*, Nice, 2007, pp. 2151-2155.

[22] T. Lu, G. Jianhua, Y. Yang, and Y. Gao, "BEP Analysis for DF Cooperative Systems Combined with Signal Space Diversity," *IEEE Commun. Letters*, vol. 16, no. 4, pp. 486-489, April 2012.

[23] T. Hashimoto and N. Suehiro, "Constellation Rotated Vector OFDM and Its Performance over Rayleigh Fading Channels," in *IEEE Commun.*, Dresden, 2009, pp. 1-5.

[24] N. F. Kiyani, J. H. Weber, A. G. Zajr and G. L. Stuber, "Performance Analysis of a System using Coordinate Interleaving and Constellation Rotation in Rayleigh Fading Channels," in *IEEE Conf. Veh. Technol* , Calgary , 2008, pp. 1-5.

[25] K. N. Pappi, N. D. Chatzidiamantis and G. K. Karagiannidis, "Error Performance of

Multidimensional Lattice Constellations—Part I: A Parallelotope Geometry Based Approach for the AWGN Channel," *IEEE trans. on Commun.*, vol. 61, no. 3, pp. 1088-1098, April 2013.

[26] K. N. Pappi, "Error Performance of Multidimensional Lattice Constellations—Part II: Evaluation over Fading Channels," *IEEE Trans. on Commun.*, vol. 61, no. 3, pp. 1099-1110, April 2013.

[27] S. Jeon, J. Lee, I. Kyung and M. K. Kim, "Component Interleaved Alamouti Coding with Rotated Constellations for Signal Space Diversity," in *IEEE International (BMSB)*, Shanghai, 2010, pp. 1-6.

Part II

Included Papers

Paper A

SYMBOL ERROR RATE OF GENERALISED SELECTION COMBINING WITH SIGNAL SPACE DIVERSITY IN RAYLEIGH FADING CHANNELS

A. Essop and H. Xu

Submitted to SAIEE – Africa Research Journal (under review)

Abstract

This paper concerns M-ary quadrature amplitude modulation (M-QAM) with signal space diversity (SSD) in Rayleigh fading channels and generalised selection combining (GSC) reception at the receiver. The symbol error rate (SER) performance of SSD for different optimal rotation angles is firstly investigated. Secondly a theoretical SER expression in Rayleigh fading channels for M-QAM with SSD and GSC is derived. The theoretical approximation for GSC reception is confirmed via simulations. Thereafter, the diversity gain of M-QAM with SSD and GSC is also analysed. Finally the signal-to-noise ratio (SNR) gap of M-QAM with SSD is investigated between selection combining (SC) and maximal ratio combining (MRC). The findings for the SNR gap will be verified via simulations.

A.1. Introduction

Over the last decade there has been a substantial increase in the number of wireless devices that utilise wireless connectivity with a large bandwidth. This drives a demand to improve wireless communications. In wireless communications, multipath fading is one of the main factors contributing to a decrease in bit error rate (BER) and/or symbol error rate (SER). The application of diversity into a wireless communication system can play a role in improving SER and/or BER performance [1].

The use of rotated signal constellations known as signal space diversity (SSD) results in a diversity known as modulation diversity being added into a wireless communication system to improve BER or SER performance [2, 3]. SSD can be thought of as a conventional M-ary quadrature amplitude modulation (M-QAM) constellation, rotated by a certain angle. Rotating the constellation would allow any two constellation points to achieve a maximum number of distinct components (constellation coordinates) [2, 3]. With the addition of component interleaving each of the components is affected by independent fading [3, 4]. As a result SSD offers superior immunity to noise as no two points will collapse at the same time [2, 3].

Receiver diversity can also be used to improve BER or SER performance. Receive diversity effectively provides multiple signal paths. This particular diversity technique takes advantage of the low probability that deep fading is unlikely to occur simultaneously on all signal paths [1]. Maximal ratio combining (MRC) and selection combining (SC) are two commonly used techniques which take advantage of multiple paths [5]. MRC offers superior performance at the cost of high implementation complexity since the receiver needs to estimate and combine all paths. SC has a much lower implementation complexity since the receiver only needs to estimate all paths and select one path, but the low complexity of SC results in poorer performance. To tradeoff between performance and complexity a hybrid selection combining scheme can be used [1]. This hybrid selection combining scheme more commonly known as generalized selection combining (GSC), is typically applied to offer simplicity instead of optimal performance. In GSC, a subset of receive antennas are selected based on each receiver path's signal-to-noise ratio (SNR). This subset is then combined using MRC. GSC is typically expressed as GSC (L_C, L), where L is the total number of receive antennas and L_c is the number of receive antennas which are being combined ($L_c \leq L$). GSC will result in MRC when $L_c = L$ and similarly SC when $L_c = 1$.

Implementing SSD together with receiver diversity can further improve BER or SER performances when compared to a single receive antenna SSD system. Receive diversity techniques with SSD were previously considered in [6]. SSD with MRC reception in Rayleigh fading channels was presented in [6]. MRC has higher resource requirements when compared to SC, such as power consumption and processing speeds. GSC allows for MRC to be used when required or a suboptimal choice between

MRC and SC. This makes GSC more feasible, as it allows the user to select an option to favourably use the available resources. For example in portable applications, battery capacity can be a weak point. A system which applies a variable GSC, depending on bandwidth load or signal strength can save significant battery power and other system resources.

GSC is a generalized combining scheme to trade-off between performance and complexity. To the authors' best knowledge M-QAM with SSD and GSC has not been discussed in literature. This motivates us to investigate the SER performance of M-QAM with SSD and GSC reception in this paper.

In a SSD system, the BER or SER depends on the rotation angle of the constellation points. This paper focuses on two previously applied methods to derive an optimal rotation angle, namely the minimum product distance (MPD) and the design criterion [6, 7]. In this paper the design criterion refers to the criterion of minimum Euclidean distance (MED) on the compound constellation. In [7], there is no discussion or direct comparison to show us which optimal rotation angle has better BER or SER performance. The first contribution of this paper is a more direct comparison of the above two methods with simulation results to support the choice of rotation angle. BER or SER of M-QAM with SSD and MRC reception has been discussed in [6, 8].The second contribution of this paper is to extend the approach in [6] to derive a closed form expression for the SER of M-QAM with SSD and GSC reception, which has not been presented in literature.

A comparison between different methods can help one to decide which method best suits an application. It is vital to know the BER or SER performance difference between the two extreme cases of GSC, as this will allow one to correctly apply a blend between SC and MRC. Diversity analysis between the two extreme cases would theoretically provide insight on the performance difference. There has not been any recent work on the diversity analysis of SSD with MRC and SC. Should the diversity analysis result in no change, it then becomes important to analyse the signal-to-noise (SNR) gap between the two extreme cases.

Previous work showing the SNR gap between SC and MRC for conventional M-QAM has been presented in [9]. However, [9] did not provide any claims as to how SSD would influence this relationship. This also motivates us to present a diversity and SNR gap investigation for M-QAM with SSD and GSC.

The paper is organised as follows: a system model will be presented in section A.2. In section A.3 the optimal rotation angles derived from design criteria and product distance criteria are discussed and presented. The theoretical SER performance is derived in section A.4. In section A.5 the diversity gain and SNR gap are analysed. Simulation results and discussions are presented in section A.6. Finally section A.7 draws the conclusion of the paper.

A.2. System Model

We consider a two dimensional M-QAM SSD system as shown in Fig. A. 1, [6]. The information bits are firstly mapped to two conventional M-QAM symbols. These two M-QAM symbols are then rotated. Finally the rotated M-QAM symbols are interleaved prior to transmission. These can be mathematically expressed as follows: let the original constellation and the rotated constellation be denoted by S and X, respectively. The rotated M-QAM symbols are given by.

$$x_i = s_i \boldsymbol{R}^{\theta} \tag{A.1}$$

where $s_i \in S, s_i = \begin{bmatrix} s_i^I & s_i^Q \end{bmatrix}$ and $x_i \in X, x_i = \begin{bmatrix} x_i^I & x_i^Q \end{bmatrix}$. $(\cdot)^I$ and $(\cdot)^Q$ are the in-phase and quadrature components of a signal, respectively, and the rotating matrix R^{θ} is given by [6].

$$\boldsymbol{R}^{\theta} = \begin{bmatrix} cos\theta & sin\theta \\ -sin\theta & cos\theta \end{bmatrix} \tag{A.2}$$

A pair of M-QAM rotated symbols is interleaved prior to transmission. A typical pair of interleaved symbols is given by.

$$u_1 = x_1^I + jx_2^Q \tag{A.3.1}$$

$$u_2 = x_2^I + jx_1^Q \tag{A.3.2}$$

The interleaved symbols $u_i,\ i \in [1:2]$, are transmitted in two subsequent time slots by a single transmit antenna over L receive antennas. Each symbol is transmitted at different time slots; however a pair of symbols needs to be received prior to retrieving the sent symbols due to the interleaving, as de-interleaving is required.

Let the received symbols at antenna j at time slot i be denoted by r_{ij}, where $i \in [1:2], j \in [1:L]$. r_{ij} can be given by

$$r_{ij} = h_{ij} u_i + n_{ij} \tag{A.4}$$

where n_{ij} is the additive white Gaussian noise (AWGN) with distribution $CN{\sim}(0, N_0)$. h_{ij} is the fading amplitude of the channel which can be modelled according to the Rayleigh distributed random variable with distribution given by Equ. (A.5).

$$f(h_{ij}) = \frac{h_{ij}}{\sigma^2} exp\left(-\frac{h_{ij}^2}{2\sigma^2}\right) \tag{A.5}$$

where $E\left[h_{ij}^2\right] = 2\sigma^2 = 1$.

We assume that full channel state information is available at the receiver. Maximum likelihood (ML) detection is performed after the interleaved pair is successfully de-interleaved. At the receiver GSC is used to estimate the transmitted symbol. A summary of the system can be viewed in Fig. A. 1.

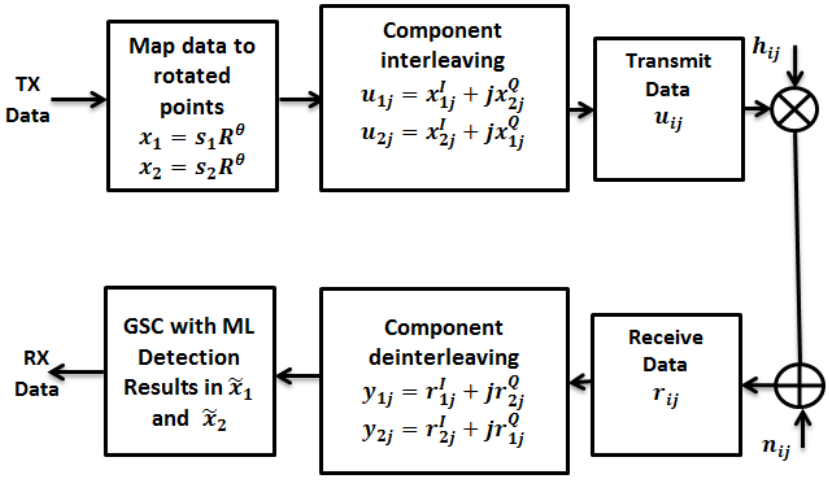

Fig. A. 1 : Summary of System Procedure

A.3. Optimal Angle of Rotation

Since the SER performance of the above system varies with the rotation angle, an optimal angle has to be found for optimal SER performance. The purpose of finding an optimal angle is to maximise the diversity which is gained from SSD. An optimal rotation angle can be determined by either maximising the MPD [2, 7, 10] or by the design criterion [7]. The optimal angles derived from the above two techniques are different. It is therefore necessary to determine which method and thus angle will result in superior performance for M-QAM with SSD system.

Current literature discusses the importance of each method used to determine an optimal angle [2, 7, 10]. The angles which have been applied in previous literature vary depending on the system and what the author wished to optimise. In [7], the authors showed that the MPD would result in superior overall performance whilst the other option results in maximising the coding gain. It is important to establish which method best suits the SER performance for M-QAM with SSD system. This section will first provide information regarding the derivation of both optimal angles. The difference in SER performance when using both optimal angles will be presented, along with how constellation size influences this difference.

The design criterion is based on rotating the constellation at an angle which ensures that every point has different in phase and quadrature components. The design criteria approach is based on maximising the MED of the expanded constellation [10, 11]. This is done by analysing the geometry

of the constellation and deriving an angle at which the MED is maximised. The basic concept of the design criterion method [7] is to ensure that each component is uniquely spaced out from each other.

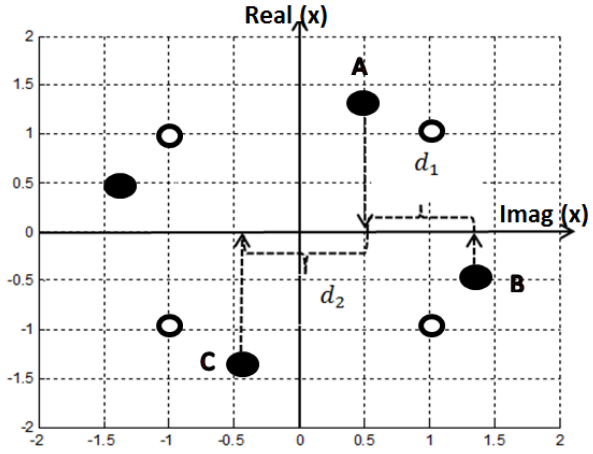

Fig. A. 2: 4-QAM Constellation to derive angle using design criteria to maximise MED.

Consider the rotated 4-QAM constellation in Fig. A. 2. The Euclidean distance between the real components of points A to B and A to C are given by d_1 and d_2, respectively. Due to symmetry by optimising this distance, all other distances are optimised. The system is optimized when $d_1 = d_2$.

An equation which represents the above criteria can be written as [10] follows.

$$d_{dc} = arg\, max_{\theta_{DC}}\{d_{min}\,(d_1\,, d_2)\} \tag{A.6}$$

Based on the above approach, the optimal angles for M-QAM can be derived and are shown in Table 1- [10]. The alternative method to determine the optimum angle is by maximising the MPD, which is given by Equ. (A.7) [2,11,12].

$$d_p = arg\, max_{\theta_{PD}} \left\{ min_{x_j \neq x_i \in X} \left| \left(x_j^I - x_i^I\right)\left(x_j^Q - x_i^Q\right) \right| \right\} \tag{A.7}$$

The optimal angles which arise from the MPD can also be derived and are also shown in Table A. 1.

Table A. 1: Rotational angles for different constellations

Constellations	**Design Criteria Approach θ_{DC} (Degrees)**	**Minimum Product distance approach θ_{PD} (Degrees)**
4-QAM	26.5624	31.7
16-QAM	14.035	31.7
64-QAM	7.1250	31.7
256-QAM	3.5763	31.7

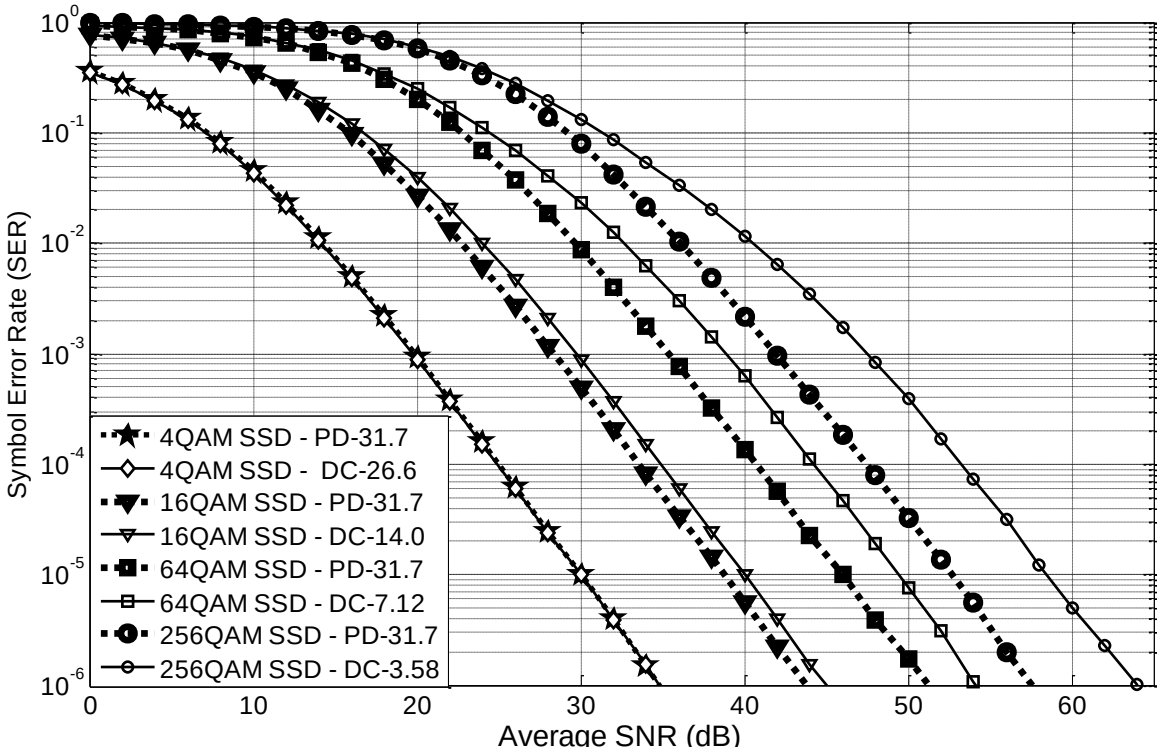

Fig. A. 3 : Simulation results for optimal angle using the two criterions

Fig. A. 3 shows the simulation results for M-QAM with SSD using a single receive antenna and the optimal angles derived from the MPD and the MED approach. The MPD criterion and MED are distinguished by the dotted and solid line, respectively.

Both the design criterion MED and MPD criterion exhibit an almost identical SER performance curve for 4-QAM. However, for 16, 64 and 256-QAM, the preferred optimal angle is the angle derived from MPD. Thus the MPD angle of 31.7 degrees will be used for all constellation sizes. As mentioned in [2], the optimisation angle of 31.7 degrees optimises the diversity which is gained. The results also depict that as the constellation size increases the SER performance difference of the system when applying each of the two angles increases. This becomes more prominent at higher M-QAM constellation sizes and at high SNR, where the difference in the two methods amounts to a SNR gap of approximately 6 dB

A.4. Performance Analysis

The SER performance of SSD systems has been investigated in previous work. The union bound and pairwise error probability (PEP) are used as techniques to evaluate the SER performance of rotated constellations in [11]. In [13], the sphere lower bound is used to evaluate the performance of rotated constellation lattices. The authors in [14] presented a combinatorial geometrical approach based on

parallel-type geometry to evaluate the performance of SSD and [15] extends this approach to multidimensional lattices. The nearest neighbour (NN) approach is used to evaluate the SER of component interleaved rotated constellations with MRC reception in [8]. Similarly to [8] the NN approach was also used to evaluate the BER of hierarchical modulated QAM with SSD in Nakagami-m fading channels with MRC reception in [11]. Due to the complexity of this system, the NN approach will be implemented in this paper to evaluate SER performance. This approach considers the nearest points to that of the test point. These nearest points are the immediate perpendicular neighbours and diagonal neighbours. This makes the theoretical equations simpler to evaluate, with negligible loss in accuracy [11].

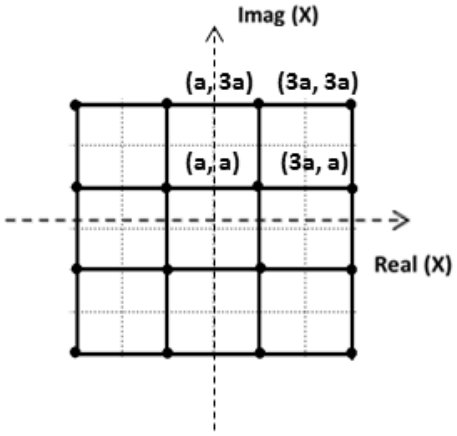

Fig. A. 4: Un-rotated constellation for 16-QAM

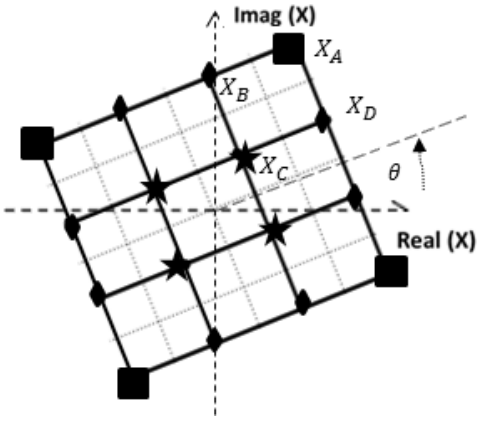

Fig. A. 5: Rotated constellation for 16-QAM

Consider Fig. A. 4.1 and Fig. A. 4.2 above, for 16-QAM, the points can be grouped into three categories: the four points at the corners X_{cor} (the square points), the eight points on the sides, X_{sid} (the diamond) and the centre four points , X_{cen} (the star points). Based on the NN approach the SER for 16-QAM can be written as follows [11]

$$P_{SER}^{16-QAM} = \frac{1}{4} P_e\,(X_{cor}) + \frac{1}{4} P_e\,(X_{cen}) + \frac{1}{2} P_e\,(X_{sid}) \tag{A.8}$$

where $P_e\,(X_{cor})$, $P_e\,(X_{cen})$ and $P_e\,(X_{sid})$ are the error probabilities of incorrectly estimating the corner, centre or side point immediate neighbours, at the respective locations shown in Fig. A. 4.2. Each of the above points will have immediate diagonal and perpendicular neighbours. Based on the NN approach only the closest perpendicular and diagonal points will be considered for the SER. Table A. 2 summarises the number of closest neighbours for each point in the respective categories.

Table A. 2: Nearest Neighbours

Points	Diagonal neighbours	Perpendicular neighbours
Side	2	3
Centre	4	4
Corner	1	2

Suppose that X_A is the transmitted symbol in Fig. A. 5. The nearest received symbols to X_A are the perpendicular X_B and X_D, and diagonal X_C. Based on $P[X_A \rightarrow X_B] = P[X_A \rightarrow X_D]$ and the NN approach the SER for rotated 16-QAM can be given as [6, 8-11]

$$P_{SER}^{16-QAM} = 3\,P[X_A \rightarrow X_B] + 2.25\;P[X_A \rightarrow X_C] \tag{A.9}$$

where $P[X_A \rightarrow X_B]$ and $P[X_A \rightarrow X_C]$ are the probabilities of an error occurring due an incorrect detection of a nearby perpendicular and diagonal point, respectively. The coordinates of X_A and X_B from Fig. A. 4 and Fig. A. 5 can be given by

$$X_A = [3a\ 3a]\begin{bmatrix} cos\theta & sin\theta \\ -sin\theta & cos\theta \end{bmatrix} \tag{A.10.1}$$

$$X_B = [a\ 3a]\begin{bmatrix} cos\theta & sin\theta \\ -sin\theta & cos\theta \end{bmatrix} \tag{A.10.2}$$

Then the Euclidean distance between X_A, X_B and X_A, X_C can be evaluated as follows.

$$d_{A\rightarrow B}^2 = 4a^2h_I^2\,cos^2\theta + 4a^2h_Q^2\,sin^2\theta \tag{A.11.1}$$

$$d_{A\rightarrow C}^2 = 4a^2h_I^2\,(1 - sin2\theta) + 4a^2h_Q^2(1 + sin2\theta) \tag{A.11.2}$$

where h_I and h_Q are two different fading channels.

Given h_I and h_Q as that fading amplitudes that the in-phase and quadrature components experience, the conditional PEP of choosing X_B given that X_A was transmitted is given by [16].

$$P[X_A \rightarrow X_B\,|h_I,\ h_Q] = Q\left(\sqrt{\frac{d_{A\rightarrow B}^2}{2N_0}}\right) \tag{A.12}$$

where $Q(\cdot)$ is the Gaussian Q function.

Substituting Equ. (A.11.1) and Equ. (A.11.2) into Equ. (A.12) results in the following.

$$P[X_A \rightarrow X_B\,|\gamma_I, \gamma_Q] = Q\left(\sqrt{\frac{1}{5}(\gamma_I\ cos^2\theta + \gamma_Q\ cos^2\theta)}\right) \tag{A.13}$$

$$P[X_A \rightarrow X_C\,|\gamma_I, \gamma_Q] = Q\left(\sqrt{\frac{1}{5}(\gamma_I\ (1 + sin2\theta)\ + \gamma_Q\ (1 - sin2\theta))}\right) \tag{A.14}$$

where $\gamma_I = SNR(h_I)^2$ and $\gamma_Q = SNR\left(h_Q\right)^2$.

The error probability $P[X_A \rightarrow X_B]$ can be obtained by averaging the conditional PEP in Equ. (A.13) over the independent fading for GSC reception as shown in Equ. (A.15).

$$P[X_A \rightarrow X_B] = \int_0^\infty \int_0^\infty P\left[X_A \rightarrow X_B \,|\gamma_I, \gamma_Q\right] f_{\gamma_I}(\gamma_I) f_{\gamma_Q}(\gamma_Q) d\gamma_I d\gamma_Q \tag{A.15}$$

where f_{γ_I} and f_{γ_Q} are the probability density functions (PDF) for GSC in Rayleigh fading channel given by Equ. (A.16) from [5, Eq. 9.325].

$$f(\gamma) = \binom{L}{L_C} \left[w_1 + \frac{1}{\bar{\gamma}} w_2\, w_3\right] \tag{A.16}$$

where $w_1 = \frac{\gamma^{L_C-1} e^{-\gamma/\bar{\gamma}}}{\bar{\gamma}^{L_C}(L_C-1)!}$, $w_2 = \sum_{l=1}^{L-L_C} (-1)^{L_C+l-1} \binom{L-L_C}{l} \left(\frac{L_C}{l}\right)^{L_C-1}$ and

$w_3 = e^{-\frac{\gamma}{\bar{\gamma}}} \left(e^{-\frac{l\gamma}{L_C\bar{\gamma}}} - \sum_{m=0}^{L_C-2} \frac{1}{m!} \left(-\frac{l\gamma}{L_C\,\bar{\gamma}}\right)^m\right)$

The trapezoidal approximation of the Q function [11], is used to simplify the above analysis and is given by

$$Q(x) = \frac{1}{2n} \left(\frac{1}{2} e^{-\frac{x^2}{2}} + \sum_{k=1}^{n-1} e^{-\frac{x^2}{2\sin^2\theta_k}}\right) \tag{A.17}$$

where $\theta_k = \frac{k\pi}{2n}$ and n is the upper limit for the summation.

The definition of a moment generating function (MGF) is given by [5].

$$M_y(s) = \int_0^\infty f_\gamma(\gamma)\; e^{s\gamma}\, d\gamma \tag{A.18}$$

The MGF for GSC in Rayleigh fading channels can be found in [17] and [5, Page 383 Equ. 9.321]

$$M_{\gamma GSC}(s) = (1 - s\bar{\gamma})^{-L_C+1} \prod_{l=Lc}^{L} \left(1 - \frac{s\bar{\gamma}L_C}{l}\right)^{-1} \tag{A.19}$$

where the average SNR $\bar{\gamma} = \mathrm{E}[\gamma_\mathrm{I}] = \mathrm{E}\left[\gamma_\mathrm{Q}\right]$, $\mathrm{E}(\cdot)$ denotes expectation.

Using Equ. (A.13) and simplifying Equ. (A.15) with the Q approximation Equ. (A.17), results in the following.

$$P[X_A \rightarrow X_B] = \int_0^\infty \int_0^\infty \{\Delta_1 + \Delta_2\} f_{\gamma_I}(\gamma_I) f_{\gamma_Q}(\gamma_Q) d\gamma_I d\gamma_Q \tag{A.20}$$

where $\Delta_1 = \frac{1}{2n} \left(0.5\, e^{-\frac{0.2\left(\gamma_I\, cos^2\,\theta + \gamma_Q\, sin^2\,\theta\right)}{2}}\right)$ and $\Delta_2 = \frac{1}{2n} \sum_{k=1}^{n-1} e^{-\frac{0.2\left(\gamma_I\, cos^2\,\theta + \gamma_Q\, sin^2\,\theta\right)}{2\sin^2\theta_k}}$.

Using Equ. (A.19), the error probability can be further simplified as.

$$P[X_A \rightarrow X_B] = \frac{1}{4n} M_{\gamma GSC}\left(-\frac{cos^2(\theta)}{\varepsilon_m}\right) M_{\gamma GSC}\left(-\frac{sin^2(\theta)}{\varepsilon_m}\right) + \frac{1}{2n}\sum_{k=1}^{n-1} M_{\gamma GSC}\left(-\frac{cos^2(\theta)}{\varepsilon_m sin^2(\theta_k)}\right) M_{\gamma GSC}\left(-\frac{sin^2(\theta)}{\varepsilon_m sin^2(\theta_k)}\right) \quad \text{(A.21)}$$

where: $\varepsilon_m = 10$.

Similarly, $P[X_A \rightarrow X_c]$ is derived as

$$P[X_A \rightarrow X_c] = \frac{1}{4n} M_{\gamma GSC}\left(-\frac{1+sin2\theta}{\varepsilon_m}\right) M_{\gamma GSC}\left(-\frac{1-sin2\theta}{\varepsilon_m}\right) + \frac{1}{2n}\sum_{k=1}^{n-1} M_{\gamma GSC}\left(-\frac{1+sin2\theta}{\varepsilon_m sin^2(\theta_k)}\right) M_{\gamma GSC}\left(-\frac{1-sin2\theta}{\varepsilon_m sin^2(\theta_k)}\right) \quad \text{(A.22)}$$

A more general expression for GSC M-QAM SSD can be written as.

$$P_{SER}^{M-QAM} = A_M P[X_A \rightarrow X_B] + B_M P[X_A \rightarrow X_c] \quad \text{(A.23)}$$

where A_M , B_M and ε_m vary with each M-QAM constellation and are tabulated in Table A.3.

Table A. 3: Values for $\mathbf{A_M}$, $\mathbf{B_M}$ **and** $\boldsymbol{\varepsilon_m}$

Constellations	$\boldsymbol{A_M}$	$\boldsymbol{B_M}$	$\boldsymbol{\varepsilon_m}$
4 - QAM	2	1	2
16 - QAM	3	2.25	10
64 - QAM	3.5	3.0625	42
256 - QAM	3.75	3.5156	170

ε_m is the average expected energy per symbol and this is calculated based on the M-QAM constellation size. The values for A_M and B_M are the numbers which relates to the constellation size. They represent respectively the number of immediate perpendicular and diagonal neighbours.

A.5. Diversity Order and SNR Gap

Diversity analysis gives an indication of the diversity of a system. The amount of diversity a communication system possesses effects the overall SER/BER performance of a communication system. The diversity order has not been analysed for M-QAM with SSD system in current literature. Thus this section will trace the analysis of diversity and SNR gap between the extreme cases of GSC which is SC and MRC.

This paper shown that GSC *($L_c \neq L$)* achieves the same diversity order as MRC for conventional M-QAM due to the diversity analysis. However the SER performance of GSC is worse than MRC [9]. There is in fact an SNR gap between GSC and MRC even in conventional M-QAM. The SNR gap between SC and MRC in Nakagami-m fading channels has been investigated in [9]. However, it has not commented on the SNR gap between SC and MRC for M-QAM with SSD. In this section the same approach proposed in [9] will be used to investigate the SNR gap for M-QAM with SSD.

A.5.1. Diversity Order

Consider that the fading is identically distributed with the same fading parameters and the same average SNR $\bar{\gamma}$ for all L_c channels. For the purpose of this paper the diversity gain for the extreme cases will be derived. The extreme cases are $L_c = 1$ and $L_c = L$, which are the SC and MRC case, respectively. The diversity order G of a communication system can be defined as the slope of its error probability $P_e(\text{SNR})$ in log-scale at values where the SNR tends to infinity [18], which can be calculated as follows [18]

$$G = lim_{\bar{\gamma}\to\infty} \frac{log[P_e(\bar{\gamma})]}{log(\bar{\gamma})} \tag{A.24}$$

When $L_c = 1$, GSC becomes SC and the PDF of SC in Rayleigh fading is given by [5]:

$$P_{\gamma}(\gamma) = \frac{L}{\bar{\gamma}} \sum_{l=0}^{L-1} (-1)^l \begin{bmatrix} L-1 \\ l \end{bmatrix} e^{-\gamma \frac{1+l}{\bar{\gamma}}} \tag{A.25}$$

The SER is largely dependent on the MED. Since most errors are caused by only the perpendicular closest neighbour and not the diagonal neighbour at high SNR the SER performance of M-QAM are greatly affected by the nearest neighbour. Therefore for diversity analysis, the SER can be simplified so that it only considers SER introduced by $P[X_A \rightarrow X_B]$.

This above assumption is validated in Fig. A. 6 and Fig. A. 7. In Fig. A. 6 the dotted line represents the theoretical SER which takes into account both $P[X_A \rightarrow X_B]$ and $P[X_A \rightarrow X_c]$ for that of an arbitrary M-QAM system, while the solid line represent the same SER expression, but with the assumption that $P[X_A \rightarrow X_C] \cong 0$. Fig. A. 6 and Fig. A. 7 illustrates this assumption for 4 and 256-

QAM SSD respectively, each applying GSC with $L_c = 3$ and $L = 3$. The difference in SNR when considering the diagonal neighbours and when neglecting the diagonal neighbours is only 0.5 dB whilst operating at 97.5 dB Fig. A. 7 illustrates the same effect for that of 256-QAM SSD.

This translates to an accuracy error for 4-QAM and 256-QAM of 0.51 % as can be seen in Equ. A.26.1 and Equ. A.26.2 respectively.

$$\frac{0.5}{97} \cong 0.51\ \% \tag{A.26.1}$$

$$\frac{0.5}{97.5} \cong 0.51\ \% \tag{A.26.2}$$

The difference of 0.5 dB remains constant at all high SNR values for all M-QAM. This validates the above statement, that at high SNR values the diagonal immediate neighbour has a negligible effect on performance. Since the diversity gain is analysed when the SNR tends to infinity the need for considering $P[X_A \rightarrow X_C]$ is negligible.

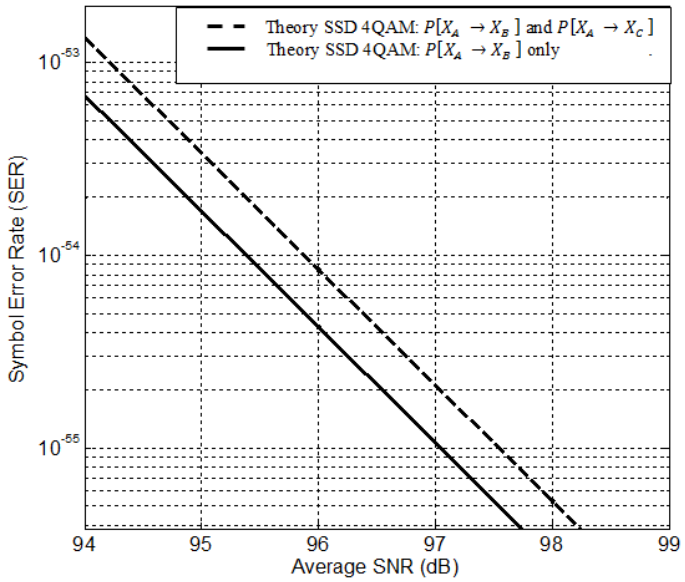

Fig. A. 6: SNR difference between using full SER expression or $P[X_A \rightarrow X_B]$ only for 4-QAM

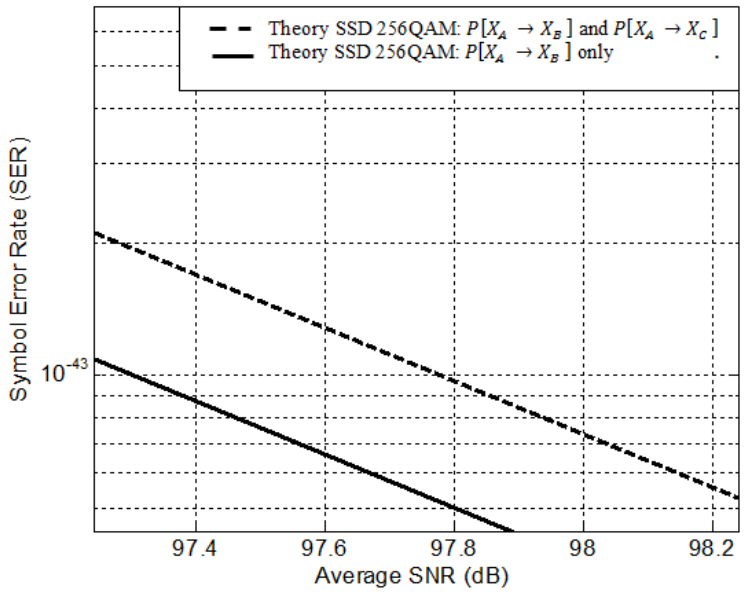

Fig. A. 7: SNR difference between using full SER expression or $\mathbf{P[X_A \rightarrow X_B]}$ only for 256-QAM

The SER is simplified by neglecting the effects of $P[X_A \rightarrow X_C]$. Based on the Chernoff bound of the Q function found in [19], Equ. (A.15) can be approximated as:

$$P[X_A \rightarrow X_B] \leq \frac{1}{2}\int_0^{\infty}\int_0^{\infty} e^{-\frac{\frac{1}{5}\left(\gamma_I \cos^2\theta + \gamma_Q \sin^2\theta\right)}{2}} f_{\gamma_I}(\gamma_I) f_{\gamma_Q}(\gamma_Q) d\gamma_I d\gamma_Q \qquad \text{(A.27)}$$

Substituting Equ. (A.25) into Equ. (A.27) results in the following:

$$P[X_A \rightarrow X_B] \leq \frac{1}{2}\int_0^{\infty} e^{-\frac{1}{5}\gamma_I \cos^2\theta} \times \frac{L}{\bar{\gamma}}\sum_{l=0}^{L-1}(-1)^l \begin{bmatrix} L-1 \\ l \end{bmatrix} e^{-\gamma_I \frac{1+l}{\bar{\gamma}}} d\gamma_I \times$$

$$\int_0^{\infty} e^{-\frac{1}{5}\gamma_Q \sin^2\theta} \times \frac{L}{\bar{\gamma}}\sum_{l=0}^{L-1}(-1)^l \begin{bmatrix} L-1 \\ l \end{bmatrix} e^{-\gamma_Q \frac{1+l}{\bar{\gamma}}} d\gamma_Q \qquad \text{(A.28)}$$

This can be simplified as follows

$$P[X_A \rightarrow X_B] \leq \frac{L!}{2}\left(\frac{1}{\prod_{l=1}^{L}\left(l+\frac{\bar{\gamma}}{5}\cos^2\theta\right)}\right) \times \left(\frac{L!}{\prod_{l=1}^{L}\left(l+\frac{\bar{\gamma}}{5}\sin^2\theta\right)}\right) \qquad \text{(A.29)}$$

So the SER approximation for 16-QAM which neglects the effects of the diagonal points is as follows

$$P_{SER} \approx A_M\, P[X_A \rightarrow X_B] = 0.5 A_M (L!)^2 \left(\frac{1}{\prod_{l=1}^{L}\left(l+\frac{\bar{\gamma}}{5}\cos^2\theta\right)}\right) \times \left(\frac{1}{\prod_{l=1}^{L}\left(l+\frac{\bar{\gamma}}{5}\sin^2\theta\right)}\right) \qquad \text{(A.30)}$$

Using the definition of the diversity order in Equ. (A.24) we have the diversity order of SC as

$$G_{SC} = lim_{\bar{\gamma}\rightarrow\infty} \frac{log\left[A_M\, P(X_A \rightarrow X_B)^{M-QAM}\right]}{log(\bar{\gamma})} = -2L \qquad \text{(A.31)}$$

When $L_c = L$, GSC becomes MRC and the PDF of MRC in Rayleigh fading is given by [5]:

$$f(\gamma) = \frac{\gamma^{L-1}\, e^{-\frac{\gamma}{\bar{\gamma}}}}{\bar{\gamma}^{L}\,(L-1)!} \tag{A.32}$$

Similar to the diversity order derivation of SC we find the diversity order of MRC to be:

$$G_{MRC} = lim_{\bar{\gamma}\to\infty} \frac{log\left[A_M\, P(X_A \to X_B)^{M-QAM}\right]}{log(\bar{\gamma})} = -2L \tag{A.33}$$

Considering the results of the diversity analysis we see that both MRC and SC have the same result. This is due to the SER difference becoming negligible as the SNR approaches infinity. This means that the diversity which is gained between SC and all GSC cases will always be the same, as proved by the extreme cases of SC and MRC as GSC is based on combining a subset of receivers, whilst MRC is based on combining all available receivers.

It becomes important to perform a SNR gap analysis between the two extreme cases of SC and MRC to provide insight on the performance differences between SC and MRC and hence GSC. The extreme cases resulted in a diversity order of -2L each. In the next subsection the SNR gap between SC and MRC will be derived.

A.5.2. SNR Gap

An SNR gap is defined in [9] as the difference in SNR or power that is required for that of SC and GSC to achieve the same SER when the diversity order is the same. At high SNR this gap will be constant since the slope of the SER for both SC and MRC/GSC is invariant. This paper will derive and discuss the SNR gap for SC and MRC. Adopting the approach proposed in [20], the SNR gap, can be determined by the following expressions

$$SER^{MRC}(\bar{\gamma}) = SER^{SC}(\bar{\gamma}\, G_m) \tag{A.34}$$

where G_m is the SNR gain.

$$SNR\ gap = 10\, log\, G_m \ \ dB \tag{A.35}$$

Similar to the diversity order analysis of section A.5.1, we only consider the errors introduced by the perpendicular point errors. The exact SER equation presented in this paper is of high complexity and hence a closed form approximation is used to solve for the SNR gap. An approximation of the Q function shown in Equ. (A.36) [21], will be used to derive the SER of $L_c = L$ and $L_c = 1$ which corresponds to the extreme cases of GSC.

$$Q(x) \approx \frac{1}{12} exp\left(-\frac{x^2}{2}\right) + \frac{1}{4} exp\left(-\frac{2x^2}{3}\right) \tag{A.36}$$

Using the PDF of SC (25) and the Q approximation Equ. (A.36) to simplify Equ. (A.15) results in the following.

$$P[X_A \rightarrow X_B] = \left(\int_0^{\infty}\left(\frac{1}{12}e^{-\frac{A}{2}} + \frac{1}{4}e^{-\frac{2A}{3}}\right)\frac{L}{\bar{\gamma}}\sum_{l=0}^{L-1}(-1)^l\begin{bmatrix} L-1 \\ l \end{bmatrix}e^{-\gamma_I\frac{1+l}{\bar{\gamma}}}d\gamma_I\right) \times \left(\int_0^{\infty}\left(\frac{1}{12}e^{-\frac{B}{2}} + \frac{1}{4}e^{-\frac{2B}{3}}\right)\frac{L}{\bar{\gamma}}\sum_{l=0}^{L-1}(-1)^l\begin{bmatrix} L-1 \\ l \end{bmatrix}e^{-\gamma_I\frac{1+l}{\bar{\gamma}}}d\gamma_I\right) \quad \text{(A.37)}$$

where $A = \frac{2}{\varepsilon_X}\cos^2\theta$ and $B = \frac{2}{\varepsilon_X}\sin^2\theta$.

Using the same SER approximation which neglects the effects of the diagonal points and evaluating the integral above Equ. (A.37), gives

$$SER^{SC} = A_m \cdot P_{SC}^1 \cdot P_{SC}^2 \quad \text{(A.38)}$$

where

$$P_{SC}^1 = \frac{A_m}{12}\left(\frac{L}{\bar{\gamma}}\sum_{l=0}^{L-1}(-1)^l\begin{bmatrix} L-1 \\ l \end{bmatrix}\frac{\bar{\gamma}}{\left(1+l+\frac{A\bar{\gamma}}{2}\right)}\right) + \frac{1}{4}\left(\frac{L}{\bar{\gamma}}\sum_{l=0}^{L-1}(-1)^l\begin{bmatrix} L-1 \\ l \end{bmatrix}\frac{\bar{\gamma}}{\left(1+l+\frac{2A\bar{\gamma}}{3}\right)}\right) \quad \text{and}$$

$$P_{SC}^2 = \frac{A_m}{12}\left(\frac{L}{\bar{\gamma}}\sum_{l=0}^{L-1}(-1)^l\begin{bmatrix} L-1 \\ l \end{bmatrix}\frac{\bar{\gamma}}{\left(1+l+\frac{B\bar{\gamma}}{2}\right)}\right) + \frac{1}{4}\left(\frac{L}{\bar{\gamma}}\sum_{l=0}^{L-1}(-1)^l\begin{bmatrix} L-1 \\ l \end{bmatrix}\frac{\bar{\gamma}}{\left(1+l+\frac{2B\bar{\gamma}}{3}\right)}\right)$$

Similarly we have:

$$SER^{MRC} = A_m \cdot P_{MRC}^1 \cdot P_{MRC}^2 \quad \text{(A.39)}$$

where $P_{MRC}^1 = \frac{A_m}{12}\left(\left(\frac{1}{\bar{\gamma}A*\frac{1}{2}+1}\right)^L + \frac{1}{4}\left(\frac{1}{\bar{\gamma}A*\frac{2}{3}+1}\right)^L\right)$ and $P_{MRC}^2 = \frac{A_m}{12}\left(\left(\frac{1}{\bar{\gamma}B*\frac{1}{2}+1}\right)^L + \frac{1}{4}\left(\frac{1}{\bar{\gamma}B*\frac{2}{3}+1}\right)^L\right)$

By comparing the terms found in Equ. (A.38) and Equ. (A.39) a simplification can be made. P_{MRC}^1 can be compared directly to P_{SC}^1 and the same applies to P_{MRC}^2 with P_{SC}^2. This simplification can be used to evaluate Equ. (A.34) which results in the following

$$\left(\frac{1}{\frac{1}{2}\bar{\gamma}B+1}\right)^L = \left(\frac{L}{\bar{\gamma}}\sum_{l=0}^{L-1}(-1)^l\begin{bmatrix} L-1 \\ l \end{bmatrix}\frac{\bar{\gamma}}{\left(1+l+\frac{BG_m\bar{\gamma}}{2}\right)}\right) \quad \text{(A.40)}$$

Using basic mathematics, from Equ. (A.40) the value of G_m can be determined as

$$G_m = (L!)^{\frac{1}{L}} \quad \text{(A.41)}$$

$$SNR\ gap_{SC-MRC} = \frac{10}{L}\log(L!)\ \ dB \quad \text{(A.42)}$$

The same result was obtained in [20]. This proves that the SNR gap is not related to the rotation angle or constellation size. Thus the SNR gap between a rotated and non-rotated constellation will be equal. Since the SC–MRC SNR gap is angle independent, the SNR gap for other cases of SC–GSC SNR gap is also. Hence a more general expression for the SNR gap between SC and GSC can be simplified for Rayleigh fading channel directly from [20]:

$$SNR\ gap_{SC-GSC} = \frac{10}{L}\log(L_c!\ \ (L_c)^{L-L_c})\ \ dB \tag{A.43}$$

where $L_c \leq L$.

The above expression provides the SNR gap for any SC to GSC system for different values of L_c. In [20], the result was derived for non-rotated constellations, but since Equ. (A.42) for the MRC case proved the derivation to be angle independent, Equ. (A.43) can be used directly for other GSC values for rotated constellations. Furthermore (A.43) does not contain any angle or constellation size dependent variables; this concisely proves the above statement.

Equ. (A.42) is verified by comparing simulation results with the expressions evaluation. Similarly Equ. (A.43) is also verified by simulation results. Both figures can be viewed in the results section.

A.6. Results

The aim of this section is to validate the theoretical derivations produced in this paper by means of simulations. The SER performance for rotated constellations of 4, 16, 64 and 256-QAM, at the optimal angle of 31.7°, for $L_c = 1,\ 2, 3$ and $L = 3$ is presented. Please note the extreme cases of MRC and SC at the extreme ends of GSC is also presented in the results, i.e. $L_c = 1$ and $L_c = 3$.

The full SER expression given by Equ. (A.23) is graphed for each case above and compared to simulation results. This will be a means to verify the mathematical expression as well as compare how good the system performs compared to what we would expect.

The simulated SNR gap of SC and MRC, is presented, to verify Equ. (A.42). The SNR gap between SC and MRC for $L = 1{:}5$ is verified in the results section via simulations. Thereafter the SNR gap for SC and GSC ($L_c = 1{:}L$) will be graphed for values of $L = 3{,}5$ to verify Equ. (A.43). The SNR gap provides more insight as to the performance compromise when switching from MRC to a specific GSC case. It would allow one to visualise the gain/loss in performance as the L_c value is increased or decreased.

The SER simulations were performed over independent and identically distributed (i.i.d) Rayleigh flat fading channels with AWGN and perfect channel estimation at the receiver.

A.6.1 SER of M-QAM with SSD in Rayleigh fading

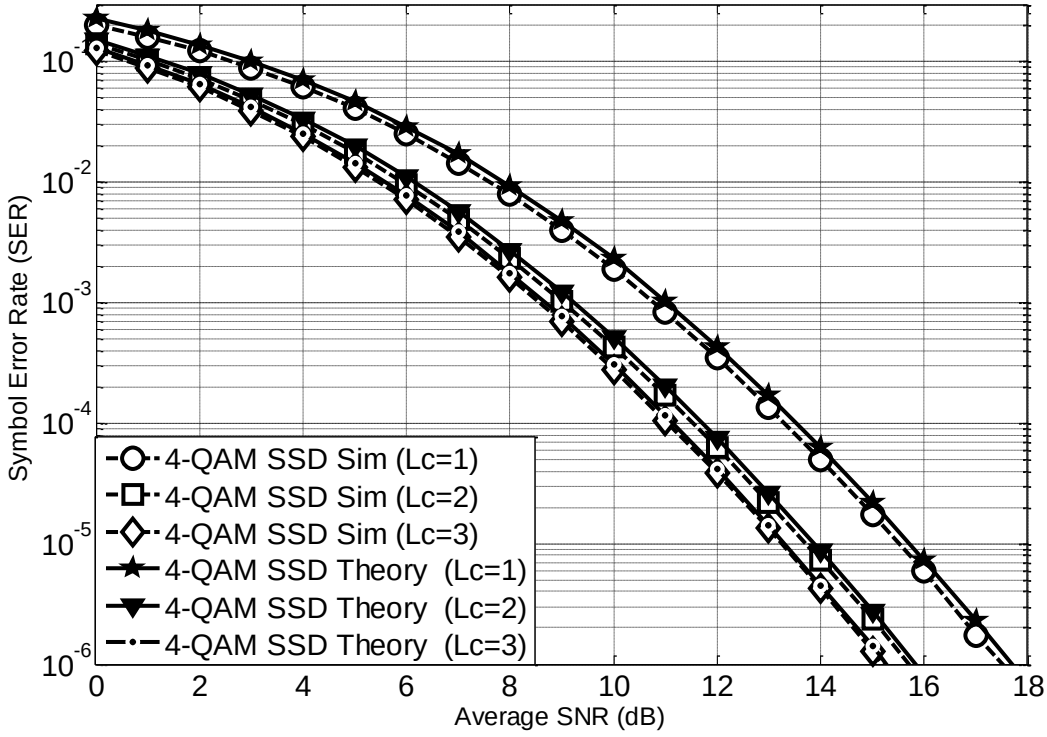

Fig. A. 8: SER - 4-QAM SSD with GSC in Rayleigh fading channel

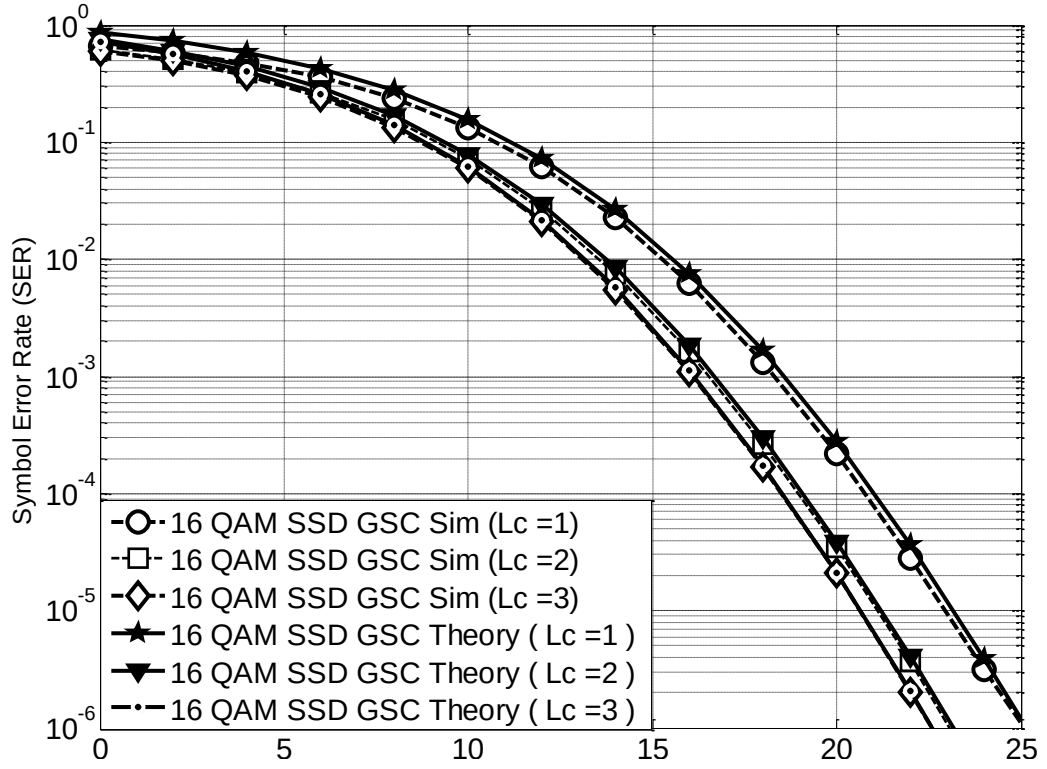

Fig. A. 9: SER - 16-QAM SSD with GSC in Rayleigh fading channel

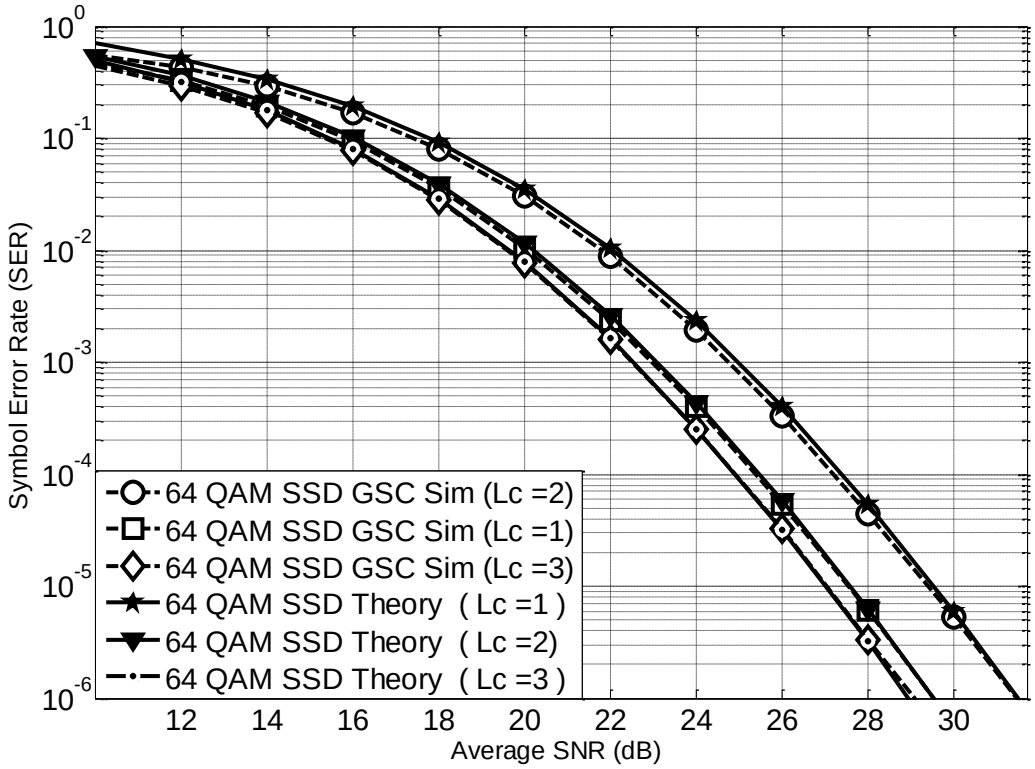

Fig. A. 10: SER - 64-QAM SSD with GSC in Rayleigh fading channel

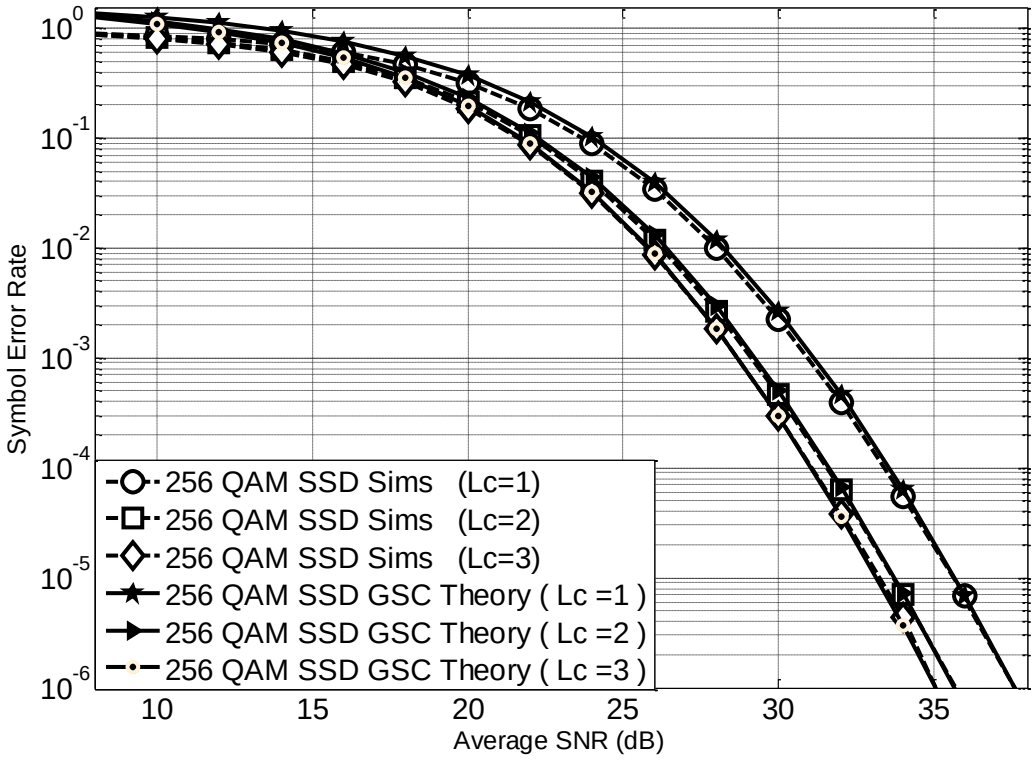

Fig. A. 11: SER - 256-QAM SSD with GSC in Rayleigh fading channel

Fig. A. 8 - Fig. A. 11 shows the simulated and theoretical SER performance of SSD systems with $L = 3$ and different L_c values for 4, 16, 64, and 256-QAM, respectively. All exhibit a small difference in performance between the simulation results of the SER and the theoretical SER at low SNR values (SNR < 17 dB). If more than a single bit error occurred this will still count as a single SER and hence a slight difference in the theory vs. simulations at low SNR values. At medium to high SNR the theoretical SER and simulation SER, for M-QAM in all GSC cases, closely overlap each other. This difference becomes more prominent as the constellation size increases because higher order constellations produce a greater number of errors at low SNR values and hence in practical applications the lower SNR values are seldom used, making the difference at lower SNR values unimportant. .

Also noticed is a performance improvement as L_c increases from SC to MRC. By utilising a GSC scheme a designer can use this information to decide on a suitable L_c value for a device.

A.6.2 SNR gap relationship

The theoretical SNR gap using Equ. (A.42) and Equ. (A.43) are compared to actual simulation results. Due to the fact that the SNR gap is constellation size independent, the simulation results are only analysed for a 16-QAM constellation size at the optimal angle of 31.7 degrees.

Fig. A.12 shows the results for the SNR gap which has been derived in section A.5.2. From Fig. A 10 one can observe that the simulation results closely overlap the theoretical results, confirming that the relationship is true. As the number of receive antennas is increased the SNR gap between SC and MRC will increase at the same rate for M-QAM with and without SSD. The simulations were performed at a constant SER of 10^{-7}, for that of SC and MRC and the dB difference is calculated and graphed for different number of receive antennas. At high SNR values the SER will be very small, thus making it hard to simulate. The relationship which was derived in section A.5.2 holds when the SNR is substantially large (SER is low at high SNR). It is then that the SER of SC and MRC will be parallel to each other and hence a constant SNR gap between them. Due to computational requirements and accuracy when simulating at low SER, the SNR gap has been graphed up to five receive antenna.

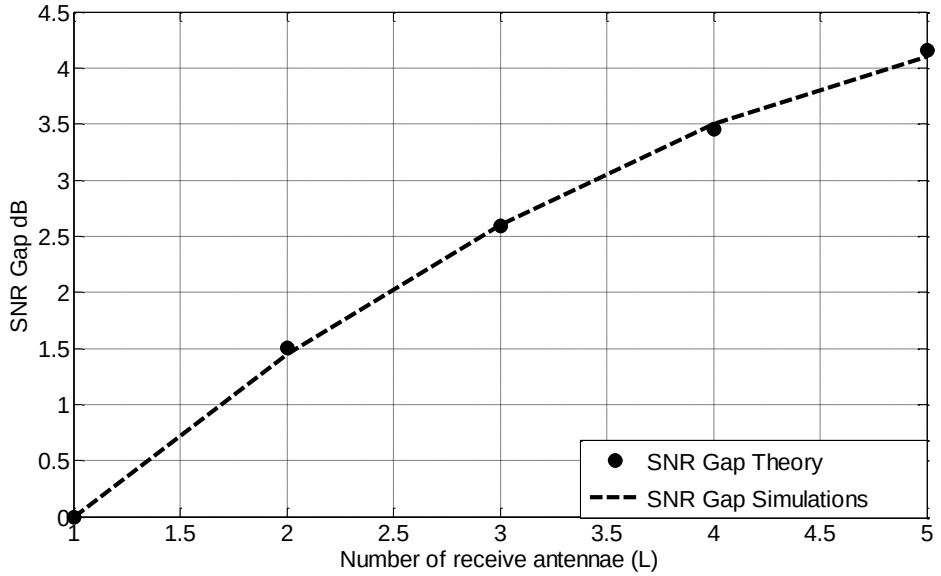

Fig. A. 12: SNR gap for different $\boldsymbol{L}$ values (MRC- SC)

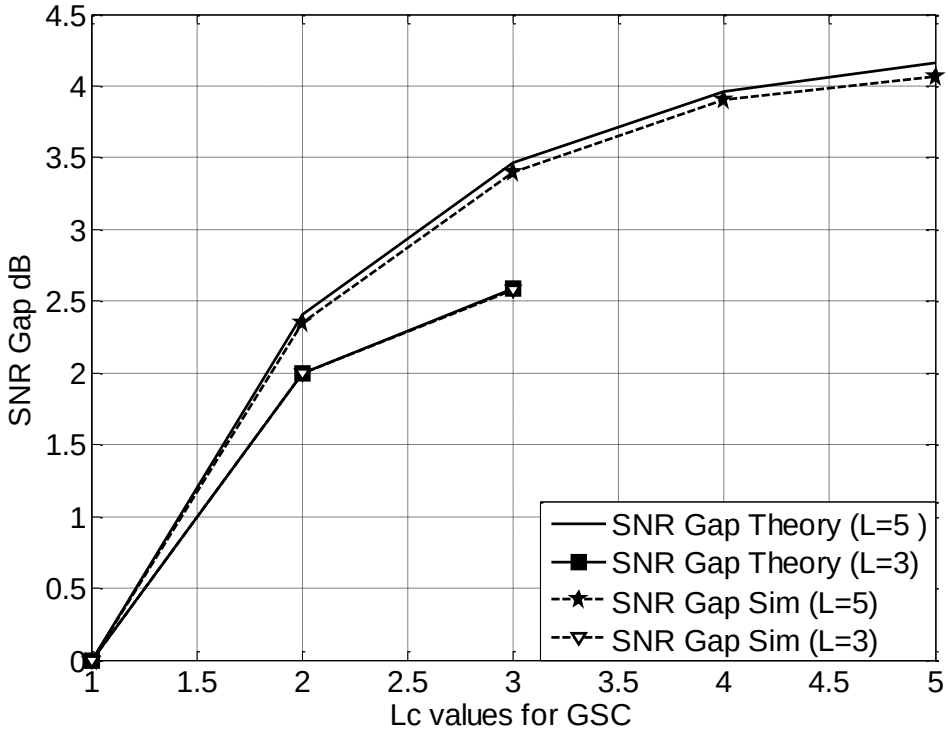

Fig. A. 13: SNR gap for different $\boldsymbol{L_c}$ values at $\boldsymbol{L = 3, 5}$

A non-linear curve representing the SNR gap between SC and MRC can be observed in Fig. A.12. From the graph one can observe that when $L = 2$ the SNR gap is 1.5 dB but when $L = 5$ the difference is 4.1 dB

Fig. A.13 illustrates the SNR gap for different L_c values when $L=5$ and $L=3$. This is to verify that Equ. (A.43) from [20] is correct. As can be seen the SNR gap increases as L_c increases. The graph gives a visual representation of the SNR gap which is gained when switching from SC to GSC and then to MRC. As can be seen the relationship is a curve which has the least SNR gap gains when L_c approaches L. For example with $L=5$ and $L_c = 2$ there is an increase in the SNR gap of 2.4 dB from that of $L_c = 1$ (SC). But when $L_c = 5$ there is an increase of 0.2 dB from that of $L_c = 4$. This is useful information as one is able to realize that even though MRC is the best performing, it might not be worth the extra complexity.

A.7. Conclusion

The use of GSC on a SSD system is presented in this paper as a possible method to improve reliable communication. The SER performance of SSD using GSC with L receive antennas is derived in Rayleigh fading based on the nearest neighbour approach. A closed form solution based on the MGF function was presented in this paper.

The relationship between applying GSC ($L_c = 1$) - SC or GSC ($L_c = L$) - MRC is derived and proved to be positively related to the number of receive antennas. Similarly the power gain between SC and MRC and hence SC and GSC are presented in this paper and proved to be positively related to the number of receive antennas. GSC proved to be useful as illustrated by the SNR gap curve and the small increase in performance as L_c approaches L. This was demonstrated by the small increase in SNR gap as L_c approaches L. The scheme presented in the paper proved to be successful as it is demonstrated that the theoretical performance closely matches the simulated performance.

A.8. References

[1] H. Xu, "Symbol Error Probability for Generalized Selection Combining," *SAIEE Research Journal*, vol. 100, no. 3, pp. 68-71, Sept 2009.

[2] J. Boutros and E. Vitebro, "Signal Space Diversity: A Power-and Bandwidth- Efficient Diversity Technique," *IEEE Trans. on Info. Theory*, vol. 44, no. 4, pp. 1453 - 1467, July 1998.

[3] J. Kim and I. Lee, "Analysis of Symbol Error Rates for Signal Space Diversity in Rayleigh Fading Channels," in *IEEE International Conf. on Commun.*, Beijing, 2008, pp. 4621 - 4625.

[4] A. Chindapol, "Bit-interleaved coded modulation with signal space diversity in Rayleigh fading," in *Signals, Systems and Computers Conf.* , Pacific Grove, CA, 1999, pp. 1003-1007.

[5] M. S Alouini and M. K. Simon, *Digital Communications over Fading Channels: A Unified Approach to Performance Analysis*.: A Wiley- Interscience Publication, 2000.

[6] Z. Paruk and H. Xu, "Performance Analysis and Simplified Detection for Two - Dimensional Signal Space Diversity," *SAIEE Africa Research Journal*, vol. 104, no. 3, pp. 97-106, September 2013.

[7] S. A. Ahmadzadeh, "Signal space cooperative communication," *IEEE Trans. on wirless Commun.*, vol. 6, no. 4, pp. 1266-1271, April 2010.

[8] S. Jeon, I. Kyung, and M. K. Kim, "Component- Interleaved receive MRC with Rotated Constellation for Signal Space Diversity.," in *IEEE Conf. Veh. Technol.*, Alaska, 2009, pp. 1-6.

[9] N. Kong and L. B. Milstein, "Simple Closed Form Aymtotic Symbol Error Rate of Selection Combining and its Power Loss Compared to the Maximal Ratio Combining over Nakagami M Fading Channels," *IEEE Trans. on Commun.*, vol. 58, no. 4, pp. 1142-1150, April 2010.

[10] S. A. Ahmadzadeh, A. K. Khandani, and S.A. Motahari, "Signal Space Cooperative Communication for Single Relay Model," University of Waterloo, Ontario, Canada., Technical Report 2009.

[11] A. Saeed, T. Quazi, and H. Xu, "Hierarchical modulated quadrature amplitude modulation with signal space diversity and maximal ratio combining reception in Nakagami-m fading channels," *IET Commun.*, vol. 7, no. 12, pp. 1296-1303, Aug 2013.

[12] G. Taricco and E. Viterbo, "Performance of component interleaved signal sets for fading channels," *Electronic letters*, vol. 32, no. 13, pp. 1170-1172, April 1996.

[13] I. Guillen, A. Fabregas, and E. Viterbo, "Sphere Lower Bound for Rotated Lattice Constellations in Fading Channels," *IEEE Wireless Commun.*, vol. 32, no. 13, pp. 1170-1172, April 1996.

[14] K. N. Pappi, N. D. Chatzidiamantis, and G. K. Karagiannidis, "Error Performance of Multidimensional Lattice Constellations—Part I: A Parallelotope Geometry Based Approach for the AWGN Channel," *IEEE Trans. on Commun.*, vol. 61, no. 3, pp. 1088-1098, April 2013.

[15] K. N. Pappi, "Error Performance of Multidimensional Lattice Constellations—Part II: Evaluation over Fading Channels," *IEEE Trans. on Commun.*, vol. 61, no. 3, pp. 1099-1110, April 2013.

[16] M. Salehi and J. G. Proakis, *Digital Communications*, 5th ed. San Diago, USA: McGraw - Hill Higher Education, 2007.

[17] M. S. Alouini and M .K. Simon, "An MGF -Based Performance Analysis of Generalized Selection Combining over Rayleigh Fading Channels," *IEEE Trans. on Commun.*, vol. 48, no. 3, pp. 401-415, March 2000.

[18] H. Dai, H. Zhang, Q. Zhou, and B. L. Hughes, "On the Diversity Order of Transmit Antenna Selection for Spatial for Spatial Multiplexing Systems ," in *Global Telecommunications Conf.* , St. Louis, Missouri , 2005, pp. 1451-1455.

[19] U. Madhow, *Fundamentals of Digital Communication*. United Kingdom : University Press , 2008.

[20] N. Kong, S. Diego, J. C. Corp, and C. Wang, "Simple BER Approximations for Generalized Selection Combining (GSC) over Rayleigh Fading Channels," in *Military Commun. Conf.* , 2006, 2006, pp. 1-5.

[21] M. Chiani, D. Dardari, and M. K. Simon, "New exponential bonds and approximations for the computation of each error probability in fading channels," in *IEEE Wireless Commun.*, vol. 2, 2003, pp. 840-845.

Paper B

ALAMOUTI CODED M-QAM WITH SINGLE AND DOUBLE ROTATED SIGNAL SPACE DIVERSITY AND GENERALISED SELECTION COMBINING RECEPTION IN RAYLEIGH FADING CHANNELS

A. Essop and H. Xu

Prepared for submission

Abstract

This paper presents Alamouti coded M-ary Quadrature amplitude modulation (M-QAM) with single and double signal rotated space diversity (SSD) and generalized selection combining (GSC) in Rayleigh fading channels. The symbol error rate (SER) performance of M-QAM with Alamouti coded single SSD and GSC is derived and presented in this paper. A moment generating function (MGF) approach is used to simplify a closed form SER expression. The use of double rotated constellations is also investigated. Simulations of Alamouti coded SSD with single and double rotation using GSC reception are compared to each other.

B.1. Introduction

The demand for enhanced wireless communications is perpetually increasing at an exponential rate as new devices utilise large quantities of bandwidth and often require a low latency connection to maintain services such as high quality video calls. Improved wireless communication systems are therefore required and the reduction in symbol error rate (SER) can lead to better communication links. This can be achieved by combating the effects of multipath fading via the introduction of diversity into a communication system [1, 2].

There are various methods to introduce diversity into a system. The use of multiple-input multiple-output (MIMO) systems is a common method employed to increase spatial diversity. Spatial diversity provides multiple replicas of the same signal travelling through uncorrelated channels [3].

Multiple receive antennas are typically combined using three popular techniques namely: maximal ratio combining (MRC), selection combining (SC) and generalized selection combining (GSC) [1, 4]. MRC combines the signals from all receive antennas and is hence the best performing of the three methods. This comes at the cost of high detection complexity. SC involves choosing the best receive antenna based on the greatest signal-to-noise ratio (SNR). It has the lowest detection complexity and results in the poorest performance. GSC selects L_C out of L branches based on largest SNRs and then combines these signals. GSC offers a solution between the two extreme cases: MRC ($L_C = L$) and SC ($L_C = 1$) [1]. GSC is generally expressed as GSC (L_C, L), where ($L_c \leq L$).

A two- branch transmitter diversity system, Alamouti space-time block coding (STBC), was proposed in [5]. Alamouti (STBC) requires the use of two transmit antennas and two time slots [6, 7]. An advantage of employing Alamouti (STBC) is in the addition of transmit diversity without any physical impact on the size and power requirements of receivers. For the purpose of this paper Alamouti coded M-QAM will be abbreviated as Alamouti coded M-QAM.

Signal space diversity (SSD) is another diversity technique which can be applied without sacrificing bandwidth or power [7]. Furthermore SSD does not require additional antennas or physical hardware. It involves rotating a signal constellation about a certain angle [7, 8]. Single rotated SSD was considered in [6, 8, 9, 10] as a method to improve SER or bit error rate (BER) performance. SSD is not only confined to single rotated constellations therefore leading to double rotated constellations being investigated. In [11], a double rotated SSD system was considered to provide communication advances in digital terrestrial video next generation handheld (DVB-NGH) by improving the BER performance.

Alamouti space-time block coded modulation with SSD was previously considered in [6] and [9]. Alamouti space-time block coded hierarchal modulation with SSD and MRC is presented in [6] whilst Alamouti space-time block coded conventional modulation with SSD and MRC is presented in [9].

To the authors' best knowledge Alamouti coded M-ary quadrature amplitude modulation (M-QAM) with SSD and GSC has not been discussed in current literature. This motivates us to investigate the SER performance of Alamouti coded M-QAM with single rotated SSD and GSC reception. Additionally Alamouti coded M-QAM with double rotated SSD and GSC reception will be investigated and its performance compared with its single rotated SSD counterpart.

This paper will be organized as follows: Alamouti coded M-QAM with single rotated SSD and GSC reception is presented in section B.2, Alamouti coded M-QAM with double rotated SSD and GSC is presented in section B.3. Section B.4 will provide simulation results and section 5 will conclude the paper, followed by appendix B1 and B2 in section B.6.

B.2. Alamouti coded M=QAM with single rotated SSD and GSC

The first system model considered in this paper is Alamouti coded M-QAM with single rotated SSD and GSC reception.

B.2.1 System model

Both single rotated SSD and Alamouti coded conventional M-QAM require two time slots to transmit and receive two symbols [5, 7].

In order for SSD to be realised in an Alamouti coded system, four symbols will need to be transmitted during four time slots [6, 9]. Alamouti coded M-QAM with SSD requires the assumption that during each pair of time slots the fading remains constant, i.e. over time slot pair one (time slot 1 and 2) and over time slot pair two (time slot 3 and 4) while different time slot pairs will experience independent fading. Two modulated symbol pairs will be transmitted across the two transmit antennas during each pair of time slots.

For the purpose of this analysis we assume that full channel state information (CSI) is available at the receiver. At the receiver GSC will be used to combine the signals according to the value of L_c. A summary of the procedure can be viewed in Fig. B 1.

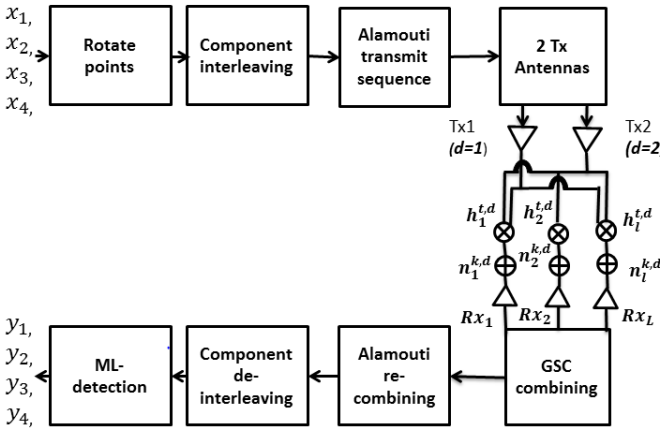

Fig. B. 1: Summary of system procedure.

Let the original data symbols and the rotated symbols be denoted by X and S, respectively. Define the rotational matrix $\boldsymbol{R}^{\theta}$ as [12]

$$\boldsymbol{R}^{\theta} = \begin{bmatrix} cos\theta. & sin\theta \\ -sin\theta & cos\theta \end{bmatrix} \tag{B.1}$$

where θ is the rotation angle.

Applying Equ. (1) with $\theta = \theta_1$ the rotated points s_i can be written as

$$s_i = x_i \, \boldsymbol{R}^{\theta_1}, \quad i \in [1{:}\,4] \tag{B.2}$$

where θ_1 is angle of rotation, $s_i \in S, s_i = \begin{bmatrix} s_i^I & s_i^Q \end{bmatrix}$ and $x_i \in X, x_i = \begin{bmatrix} x_i^I & x_i^Q \end{bmatrix}$, $(\cdot)^I$ and $(\cdot)^Q$ are the in-phase and quadrature components of a signal, respectively.

The rotated symbols will be component interleaved as follows.

$$u_{\mathrm{i}} = s_{\mathrm{i}}^I + j s_{\mathrm{i+2}}^Q, \qquad i \in \{1{:}\,2\} \tag{B.3.1}$$

$$u_i = s_i^I + j s_{i-2}^Q, \qquad i \in \{3{:}\,4\} \tag{B.3.2}$$

Let k represent the time slot and $(*)$ represent the conjugate of a variable. Applying Alamouti coded modulation on the interleaved signals results in (u_1,u_2) and $(-u_2^*,u_1^*)$ being transmitted in the first pair of time slots ($k \in [1{:}\,2]$) while (u_3,u_4) and $(-u_4^*,u_3^*)$ being transmitted in the second pair of time slots ($k \in [3{:}\,4]$). Each pair will be transmitted using two transmit antennas and received by L receive antennas.

Let t, d and l represent the time slot pair, transmit antenna and receive antenna numbers respectively, where $t \in [1{:}\,2]$, $d \in [1{:}\,2]$ and $l \in [1 : L]$. Each receive antenna will receive data through a

frequency flat fading Rayleigh channel with additive white Gaussian noise (AWGN) with distribution $CN\{0,1\}$.

The received signals at receive antenna l during time slots $k \in [1:4]$ and time slot pairs $t \in [1:2]$ are given below.

$$r_l^1 = h_l^{1,1}u_1 + h_l^{1,2}u_2 + n_l^1 \quad \text{(B.4.1)}$$

$$r_l^2 = -h_l^{1,1}u_2^* + h_l^{1,2}u_1^* + n_l^2 \quad \text{(B.4.2)}$$

$$r_l^3 = h_l^{2,1}u_3 + h_l^{2,2}u_4 + n_l^3 \quad \text{(B.4.3)}$$

$$r_l^4 = -h_l^{2,1}u_4^* + h_l^{2,2}u_3^* + n_l^4 \quad \text{(B.4.4)}$$

where r_l^k is the received signal during time slot k at receive antenna l. $h_l^{t,d}, h_l^{t,d} = \zeta_l^{t,d}\left(e^{j\varphi_l^{t,d}}\right)$, represents the channel fading coefficient between transmit antenna d and receive antennas l during time slot pair t. The amplitude ($\zeta_l^{t,d}$) of the fading coefficient follows the Rayleigh distribution and $\varphi_l^{t,d}$ is uniformly distributed over $[0: 2\pi]$. n_l^k, $n_l^k = n_l^{k,1} + n_l^{k,2}$ is the AWGN.

Since GSC is considered in this paper the received signals for L_c branches are now combined using GSC techniques and the combining scheme given by [5, 6].

$$Cr_1 = \sum_{l=1}^{Lc}\left(h_l^{1,1}\right)^*\left(r_l^1\right) + h_l^{1,2}\left(r_l^2\right)^* \quad \text{(B.5.1)}$$

$$Cr_2 = \sum_{l=1}^{Lc} -h_l^{1,1}\left(r_l^2\right)^* + \left(h_l^{1,2}\right)^*\left(r_l^1\right) \quad \text{(B.5.2)}$$

$$Cr_3 = \sum_{l=1}^{Lc}\left(h_l^{2,1}\right)^*\left(r_l^3\right) + h_l^{2,2}\left(r_l^4\right)^* \quad \text{(B.5.3)}$$

$$Cr_4 = \sum_{l=1}^{Lc} -h_l^{2,1}\left(r_l^4\right)^* + \left(h_l^{2,2}\right)^*\left(r_l^3\right) \quad \text{(B.5.4)}$$

Component de-interleaving will be performed between the time slot pairs as per Equ. (B.6.1) and Equ. (B.6.2)

$$\widetilde{Cr_k} = Cr_{\mathrm{k}}^I + j\,Cr_{\mathrm{k+2}}^Q \quad i \in [1:2] \quad \text{(B.6.1)}$$

$$\widetilde{Cr_k} = Cr_{\mathrm{k}}^I + j\,Cr_{\mathrm{k-2}}^Q \quad i \in [3:4] \quad \text{(B.6.2)}$$

where $Cr_k = \left[Cr_k^I \;\; Cr_k^Q\right]$ and $\widetilde{Cr_k} = \left[\widetilde{Cr_k}^I \;\; \widetilde{Cr_k}^Q\right]$.

Similar to [6], maximum Likelihood (ML) detection is used to estimate the transmitted symbols using the decision rule provided in [5]. The estimated symbols [1:4] will be given by y_k, $k \in [1:4]$.

$$y_k = \arg\min_{\hat{x}_i \in S}\left\{\left(V_2\left|\widetilde{Cr_k}^I - V_1\hat{x}_i^I\right|^2\right) + \left(\left(V_1\left|\widetilde{Cr_k}^Q - V_2\hat{x}_i^Q\right|^2\right)\right)\right\} \; k \in [1:2] \quad \text{(B.7.1)}$$

$$y_k = \arg\min_{\hat{x}_i \in S}\left\{\left(V_1\left|\widetilde{Cr_k}^I - V_2\hat{x}_i^I\right|^2\right) + \left(\left(V_2\left|\widetilde{Cr_k}^Q - V_1\hat{x}_i^Q\right|^2\right)\right)\right\} \; k \in [3:4] \quad \text{(B.7.2)}$$

where $V_t = A^{t,1} + A^{t,2}$, $A^{t,d} = \sum_{l=1}^{Lc} \left| h_l^{t,d} \right|^2$, $\hat{x}_i = \left[\hat{x}_i^I \quad \hat{x}_i^Q \right], t \in [1:2], d \in [1:2]$, and $i \in [1:4]$.

SSD requires an M-QAM constellation to be rotated at a specific angle to achieve optimal performance in terms of SER. There are two commonly used techniques to derive this angle namely the minimum product distance approach and the minimum Euclidean distance approach [13]. The minimum Euclidean distance approach is based on maximising the minimum Euclidean distance between points and this is done by analysing the geometry of the constellation itself. The minimum product distance approach is based on maximising the minimum product distance. It has been shown that the minimum product distance approach results in superior overall performance [7, 13, 14]. This system will apply an optimal angle of $\theta_1 = 31.7°$ degrees derived using the minimum product distance approach given by Equ. (B.8) [7].

$$d_p = \arg\max_\theta \left\{ \min_{s_j \neq s_i \in S} \left| \left(s_j^I - s_i^I \right) \left(s_j^Q - s_i^Q \right) \right| \right\} \tag{B.8}$$

B.2.2 Performance analysis

The SER of Alamouti coded M-QAM with SSD was previously evaluated by applying the nearest neighbour (NN) approach with ML detection in [15]. In [9], the NN approach was used to evaluate the SER of a SSD system. Alamouti coded hierarchical modulated M-QAM with SSD was evaluated using the union bound NN in [6]. The authors in [16] present the exact SEP in AWGN of multidimensional signal sets using two closed form bounds namely: multiple sphere lower bound (MSLB) and multiple sphere upper bound (MSUB), whilst this approach was extended over fading channels in [17].

This paper will consider the NN approach to evaluate the SER of Alamouti coded M-QAM with SSD and GSC. The NN approach only considers the nearest perpendicular and diagonal points from that of any other point in the constellation. A similar approach was implemented, in [6, 10].

In [14], it was proved that an Alamouti two transmit antenna diversity system is mathematical equivalent to a conventional MRC system with a single transmit antennae using half the transmit power and double the receive antenna number. This section uses this relationship to evaluate the SER of this system.

Let the SER of an Alamouti coded M-QAM with SSD and GSC be denoted by $\mu(\Upsilon, L_c, L)$ and a conventional M-QAM with SSD and GSC be denoted by $\varrho(\Upsilon, L_c, L)$. A relationship between the two has been derived in [5] and is represented below in Equ. (B.9).

$$\mu(\Upsilon, L_c, L) = \varrho(\tfrac{\Upsilon}{2}, 2L_c, 2L) \tag{B.9}$$

where ϒ is the instantaneous SNR.

The SER of 16-QAM Alamouti coded SSD will be derived with aid of the relationship presented above in Equ. (B.9). This relationship will be used to evaluate the SER of this system. This system will be analysed as if it were a single transmit antenna system with double the L_c and L values and half the instantaneous SNR value. For a single transmit antenna system with SSD, the SER performance can be analysed with the assumption that the in-phase and quadrature components experience amplitude fading only.

Let $\gamma_l = \frac{E_s}{N_0}\left(h_l^{t,d}\right)^2$ be the instantaneous SNR for l^{th} branch. Then the average SNR for l^{th} branch is given by $\bar{\gamma}_l = E[\gamma_l]$, where E_s is the symbol energy. In this paper we only consider independent and identically distributed (i.i.d.) channels, therefore we have $\bar{\gamma}_l = \bar{\gamma}$.

The probability density function (PDF) for Alamouti coded M-QAM with GSC in Rayleigh fading channels has been adapted from [[4], Eq. 9.325] for Alamouti coded M-QAM by applying the relationship presented in Equ. (B.9).

$$f(\gamma) = \binom{2L}{2L_C}\left[\delta_1 + \frac{1}{0.5\bar{\gamma}}\delta_2\,\delta_3\right] \tag{B.10}$$

where

$\delta_1 = \frac{\gamma^{2L_c-1}e^{-\gamma/\frac{\bar{\gamma}}{2}}}{\left(\frac{\bar{\gamma}}{2}\right)^{L_c}(2L_c-1)!}$, $\delta_2 = \sum_{l=1}^{2L-2L_c}(-1)^{2L_c+l-1}\binom{2L-2L_c}{l}\left(\frac{2L_c}{l}\right)^{2L_c-1}$ and

$\delta_3 = e^{-\frac{\gamma}{\frac{\bar{\gamma}}{2}}}\left(e^{-\frac{l\gamma}{2L_c\frac{\bar{\gamma}}{2}}} - \sum_{m=0}^{2L_c-2}\frac{1}{m!}\left(-\frac{l\gamma}{2L_c\frac{\bar{\gamma}}{2}}\right)^m\right)$.

Similarly a moment generating function (MGF) for GSC in Rayleigh fading channels presented in [18] and [[4], Page 383 Eq. 9.321] has been adapted using Equ. (B.9) and is presented below.

$$M_{\gamma GSC_{AL}}(s) = \left(1 - s\frac{\bar{\gamma}}{2}\right)^{-2L_C+1}\prod_{l=2Lc}^{2L}\left(1 - \frac{s\bar{\gamma}2L_C}{l}\right)^{-1} \tag{B.11}$$

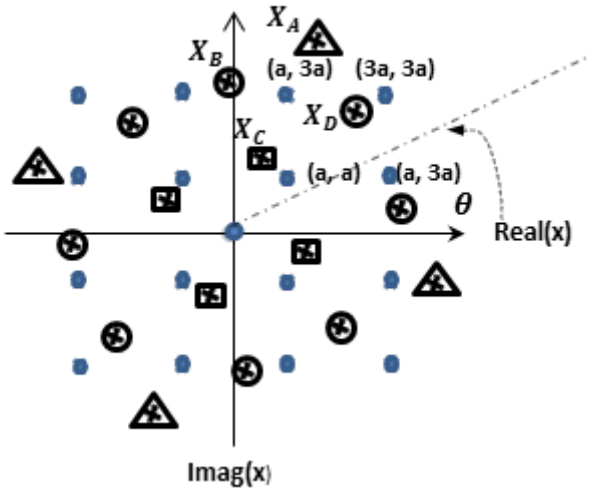

Fig. B. 2: Rotation of 16 QAM by angle **θ**

An example of a single rotated constellation can be viewed above in Fig. B 2 where ✱ and ● represent the rotated and un-rotated points of 16-QAM, respectively. Similar to [15], the points in Fig. B 2 can be divided into three categories: the four corner pints, X_{cor} (triangles), the eight points on the sides, X_{sid} (circles) and the centre four points , X_{cen} (squares).

Using the NN approach found in [3, 6, 9], the SER for Alamouti coded 16-QAM with SSD and GSC can be simplified as follows.

$$P_{SER}^{16QAM} = 3\,P[X_A \rightarrow X_B] + 2.25\;P[X_A \rightarrow X_C] \tag{B.12}$$

where $P[X_A \rightarrow X_B]$ is the probability of error of incorrectly detecting immediate perpendicular points and $P[X_A \rightarrow X_C]$ is the probability of error of incorrectly detecting immediate diagonal points.

Based on the derivation presented in [[10], Equ. (8),(12)]. The following equations are derived in Appendix B1.

$$P\left[X_A \rightarrow X_B \,|\gamma_I, \gamma_Q\right]_{AL} = Q\left(\sqrt{\tfrac{1}{5}\left(\gamma_{\mathrm{I}} \cos^2\theta_1 + \gamma_{\mathrm{Q}} \cos^2\theta_1\right)}\right) \tag{B.13.1}$$

$$P\left[X_A \rightarrow X_C \,|\gamma_I, \gamma_Q\right]_{AL} = Q\left(\sqrt{\tfrac{1}{5}\left(\gamma_{\mathrm{I}}\,(1+\sin 2\theta_1) + \gamma_{\mathrm{Q}}\,(1-\sin 2\theta_1)\right)}\right) \tag{B.13.2}$$

where $\gamma_I = SNR(h_I)^2$ and $\gamma_Q = SNR\left(h_Q\right)^2$. h_I and h_Q are the channel gains that both the in phase and quadrature components experience. For 16-QAM, $SNR = \frac{10a^2}{N_0}$.

By averaging the pairwise error probability (PEP) over independent fading channels, $P[X_A \rightarrow X_B]_{AL}$ can be evaluated with the following integral

$$P[X_A \rightarrow X_B]_{AL} = \int_0^\infty \int_0^\infty P[X_A \rightarrow X_B | \gamma_I, \gamma_Q] f_{\gamma_I}(\gamma_I) f_{\gamma_Q}(\gamma_Q) \mathrm{d}\gamma_I \mathrm{d}\gamma_Q \tag{B.14}$$

where f_{γ_I} and f_{γ_Q} represent the PDF for Alamouti coded M-QAM with GSC, Equ. (B.10).

Simplifying Equ. (B.14) using an MGF function results in the following expressions, details can be viewed in Appendix B2.

$$\begin{aligned} P[X_A \rightarrow X_B]_{AL} &= \frac{1}{4n} {M_{\gamma GSC}}^{Al}\left(-\frac{\Omega_1}{\varepsilon_M}\right) {M_{\gamma GSC}}^{Al}\left(-\frac{\Omega_2}{\varepsilon_M}\right) + \\ &\frac{1}{2n}\sum_{k=1}^{n-1} {M_{\gamma GSC}}^{Al}\left(-\frac{\Omega_1}{\varepsilon_M \sin^2(\theta_k)}\right) {M_{\gamma GSC}}^{Al}\left(-\frac{\Omega_2}{\varepsilon_M \sin^2(\theta_k)}\right) \end{aligned} \tag{B.15}$$

where $\theta_k = \frac{k\pi}{2n}$ and n is the upper limit of the summation, ε_M is the average expected energy per symbol with the values of 2, 10, 42, 170 for 4/16/64-QAM respectively. $\Omega_1 = \cos^2\theta_1$, $\Omega_2 = \sin^2\theta_1$, $\Omega_3 = (1 + \sin 2\theta_1)$, and $\Omega_4 = (1 - \sin 2\theta_1)$.

Similarly for $P[X_A \rightarrow X_C]_{AL}$, we have

$$\begin{aligned} P[X_A \rightarrow X_C]_{AL} &= \frac{1}{4n} {M_{\gamma GSC}}^{Al}\left(-\frac{\Omega_3}{\varepsilon_M}\right) {M_{\gamma GSC}}^{Al}\left(-\frac{\Omega_4}{\varepsilon_M}\right) + \\ &\frac{1}{2n}\sum_{k=1}^{n-1} {M_{\gamma GSC}}^{Al}\left(-\frac{\Omega_3}{\varepsilon_M sin^2(\theta_k)}\right) {M_{\gamma GSC}}^{Al}\left(-\frac{\Omega_4}{\varepsilon_M sin^2(\theta_k)}\right) \end{aligned} \tag{B.16}$$

Substituting Equ. (B.15) and Equ. (B.16) into Equ. (B.12) results in the SER of Alamouti coded 16 QAM with SSD and GSC.

$$P_{SER}^{MQAM}{}_{AL} = A_M P[X_A \rightarrow X_B]_{AL} + B_M P[X_A \rightarrow X_C]_{AL} \tag{B.17}$$

where $P[X_A \rightarrow X_B]_{AL}$ and $P[X_A \rightarrow X_C]_{AL}$ is given by Equ. (B.15) and Equ. (B.16), respectively. A_M is the number of perpendicular immediate neighbours. $B_M$is the number of diagonal immediate neighbours. $A_M = 2, 3, 3.5, 3.75$ and $B_M = 1, 2.25, 3.06, 3.51$ for 4/16/64-QAM , respectively.

B.3. Alamouti coded M-QAM with double rotated SSD and GSC

The system model of Alamouti coded M-QAM with double rotated SSD and GSC is presented in this section.

Double rotated SSD, consists of two rotations and two interleaving processes. For the purpose of this paper both rotations will be implemented using 31.7 ° degrees ($\theta_1 = \theta_2 = 31.7°$) . For squared M-QAM,, all rotation angles are 31.7 degrees and from a theoretical point of view it is still optimal. This will be performed using the same rotational matrix presented in Equ. (B.1) with $\theta = \theta_2$ A summary of this system can be viewed in Fig. B 3.

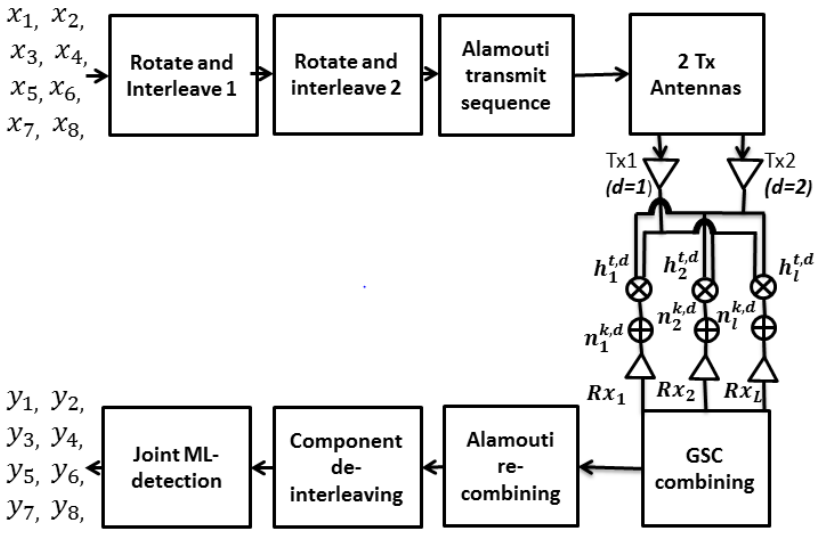

Fig. B. 3: Summary of Alamouti coded SSD with double rotation and GSC reception system

The first rotation procedure will follow directly from section B.2.1 but with eight symbols and transmitted during eight time slots. Let the original data symbols and rotation no.1 symbols be denoted by X and S. The rotated points can be computed using Equ. (B.1) with $= \theta_1$.

$$s_i = x_i \, \boldsymbol{R}^{\theta}, \qquad i \in [1:8] \tag{B.18}$$

where i is the symbol number, $s_i \in S, s_i = \begin{bmatrix} s_i^I & s_i^Q \end{bmatrix}$ and $x_i \in X, x_i = \begin{bmatrix} x_i^I & x_i^Q \end{bmatrix}$.

The first interleaving process can be written as follows.

$$u_{\mathrm{i}} = s_{\mathrm{i}}^I + j s_{\mathrm{i+2}}^Q \qquad i \in \{1,2,5,6\} \tag{B.19.1}$$

$$u_i = s_i^I + j s_{i-2}^Q \qquad i \in \{3,4,7,8\} \tag{B.19.2}$$

The interleaved data is then rotated with an angle of 31.7 ° for the second rotation.. Expanding the rotated data will result in the following

$$v_{\mathrm{i}} = v_{\mathrm{i}}^{I} + jv_{\mathrm{i}}^{Q} \qquad i \in [1:8] \tag{B.20}$$

where $v_i \in V, v_{\mathrm{i}}^{I} = u_{\mathrm{i}}^{I}\cos\theta_2 + u_{\mathrm{i}}^{Q}(-\sin\theta_2)$, $v_{\mathrm{i}}^{Q} = u_{\mathrm{i}}^{I}\sin\theta_2 + u_{\mathrm{i}}^{Q}\cos\theta_2$ and $\theta_2 = 31.7°$.

A second interleaving process is required.

$$w_{\mathrm{i}} = v_{\mathrm{i}}^{I} + jv_{\mathrm{i+4}}^{Q} \qquad i \in [1:4] \tag{B.21.1}$$

$$w_i = v_i^{I} + jv_{i-4}^{Q} \qquad i \in [5:8] \tag{B.21.2}$$

The symbols are transmitted using Alamouti coding and follows the same approach as [5], which was adapted for Alamouti coded M-QAM with single rotated SSD in section B.2.

Let t, d and l represent the time slot pair, transmit antenna and receive antenna numbers respectively, where $t \in [1:4]$, $d \in [1:2]$ and $l \in [1:L]$. Similar to Equ. (B.4.1) to (B.4.4), we have the following set of equations which represents each received signal during time slots $k \in [1:8]$ at each receive antenna l.

$$r_l^k = w_k h_l^{\lambda_1,1} + w_{k+1} h_l^{\lambda_1,2} + n_l^k \qquad k \in \{1,3,5,7\} \tag{B.22.1}$$

$$r_l^k = -(w_k^*) h_l^{\lambda_2,1} + (w_{k-1}^*) h_l^{\lambda_2,2} + n_l^k \qquad k \in \{2,4,6,8\} \tag{B.22.2}$$

where $n_l^k = n_l^{k,1} + n_l^{k,2}$ is the AWGN, $\lambda_1 = \frac{1}{2}(k+1)$ and $\lambda_2 = \frac{1}{2}(k)$.

Similar to Equ. (B.6.1) to (B.6.4) , Alamouti coded M-QAM with double rotated SSD and GSC, is combined as follows

$$Cr_k = \sum_{l=1}^{Lc} \left(h_l^{\lambda_1,1}\right)^* \left(r_l^k\right) + h_l^{\lambda_1,2}\left(r_l^{k+1}\right)^* \qquad k \in 1,3,5,7 \tag{B.23.1}$$

$$Cr_k = \sum_{l=1}^{Lc} -h_l^{\lambda_2,1}\left(r_l^k\right)^* + \left(h_l^{\lambda_2,2}\right)^* \left(r_l^{k-1}\right) \qquad k \in 2,4,6,8 \tag{B.23.2}$$

where $\lambda_1 = \frac{1}{2}(k+1)$ and $\lambda_2 = \frac{1}{2}(k)$..

In double rotated SSD only the second interleaving is recoverable and therefore one de-interleaving process is applied before ML detection.

$$\widetilde{Cr_k} = Cr_k^{I} + j\, Cr_{\mathrm{k+4}}^{Q} \qquad k \in [1:4] \tag{B.24.1}$$

$$\widetilde{Cr_k} = Cr_{\mathrm{k}}^{I} + j\, Cr_{\mathrm{k-4}}^{Q} \qquad k \in [5:8] \tag{B.24.2}$$

Due to the first interleaving process in double rotated SSD each pair of interleaved symbols remains related to each other. Consequently joint ML detection will be employed at the receiver in order to retrieve the sent data of each interleaved pair resulting in two symbols being estimated at a time. Joint

ML detection is based on estimating two symbols at the same time, $\hat{x}_i$ and $\hat{z}_i$. For example y_1 and y_3 will be estimated using $\hat{x}_i$ and $\hat{z}_i$ respectively.

$$(y_1, y_3) = \arg\min_{\substack{\hat{x}_i \in V, \\ \hat{z}_i \in V}} \left\{ \left((\acute{\rho}^1) \left| B_1^{1\,I} \right|^2 + (\acute{\rho}^3) \left| B_3^{1\,Q} \right|^2 \right) + \left((\acute{\rho}^2) \left| G_2^{3\,\mathrm{I}} \right|^2 + (\acute{\rho}^4) \left| G_4^{3\,Q} \right|^2 \right) \right\} \text{(B. 25.1)}$$

$$(y_2, y_4) = \arg\min_{\substack{\hat{x}_i \in V, \\ \hat{z}_i \in V}} \left\{ \left((\acute{\rho}^1) \left| B_1^{2\,\mathrm{I}} \right|^2 + (\acute{\rho}^3) \left| B_3^{2\,\mathrm{Q}} \right|^2 \right) + \left((\acute{\rho}^2) \left| G_2^{4\,\mathrm{I}} \right|^2 + (\acute{\rho}^4) \left| G_4^{4\,\mathrm{Q}} \right|^2 \right) \right\} \text{(B.25.2)}$$

$$(y_5, y_7) = \arg\min_{\substack{\hat{x}_i \in V, \\ \hat{z}_i \in V}} \left\{ \left((\acute{\rho}^3) \left| B_3^{5\,\mathrm{I}} \right|^2 + (\acute{\rho}^1) \left| B_1^{5\,\mathrm{Q}} \right|^2 \right) + \left((\acute{\rho}^4) \left| G_4^{7\,\mathrm{I}} \right|^2 + (\acute{\rho}^2) \left| G_2^{7\,\mathrm{Q}} \right|^2 \right) \right\} \text{(B.25.3)}$$

$$(y_6, y_8) = \arg\min_{\substack{\hat{x}_i \in V, \\ \hat{z}_i \in V}} \left\{ \left((\acute{\rho}^3) \left| B_3^{6\,\mathrm{I}} \right|^2 + (\acute{\rho}^1) \left| B_1^{6\,\mathrm{Q}} \right|^2 \right) + \left((\acute{\rho}^4) \left| G_4^{8\,\mathrm{I}} \right|^2 + (\acute{\rho}^2) \left| G_2^{8\,\mathrm{Q}} \right|^2 \right) \right\} \text{(B.25.4)}$$

where $B_t^{k\,\mathrm{I}} = \widetilde{\mathrm{C}r_k}^{\,\mathrm{I}} - V_t \hat{x}_i^{\mathrm{I}}$, $B_t^{k\,\mathrm{Q}} = \widetilde{\mathrm{C}r_k}^{\,\mathrm{Q}} - V_t \hat{x}_i^{\mathrm{Q}}$, $G_t^{k\,\mathrm{I}} = \widetilde{\mathrm{C}r_k}^{\,\mathrm{I}} - V_t \hat{z}_i^{\mathrm{I}}$, $G_t^{k\,\mathrm{Q}} = \widetilde{\mathrm{C}r_k}^{\,\mathrm{Q}} - V_t \hat{z}_i^{\mathrm{Q}}$, $\acute{\rho}^{\tau} = \sum_{t=1, t\neq\tau}^{t=4} V_t$, $V_t = A^{t,1} + A^{t,2}$, $\hat{x}_i = \left[\hat{x}_i^{I} \;\; \hat{x}_i^{Q}\right]$, , $\hat{z}_i = \left[\hat{z}_i^{I} \;\; \hat{z}_i^{Q}\right]$, $A^{t,d} = \sum_{l=1}^{Lc} \left| h_l^{t,d} \right|^2$, $t \in [1{:}\,4]$ and $d \in [1{:}\,4]$, $i \in [1{:}\,8]$.

B.4. Simulations

This section will provide information pertaining to the SER performance improvements which are realised when Alamouti coded M-QAM is combined with SSD and GSC. Monte Carlo simulations are used to validate the theoretical SER expression of Alamouti coded M-QAM with single rotated SSD and GSC. Thereafter the SER of Alamouti coding with 0, 1 and 2 rotation SSD and GSC is also is also presented.

All simulations are conducted in i.i.d. Rayleigh fading channels in the presence of AWGN as per the system model. It is assumed that full CSI is available at the receiver and that all antennas are sufficiently spaced apart to avoid any correlation between channels.

Diversity analysis gives an indication of the diversity of a system. The amount of diversity a communication system possesses effects the overall SER/BER performance of a communication system. The diversity order has not been analysed for M-QAM with SSD system in current literature. Thus this section will trace the analysis of diversity and SNR gap between the extreme cases of GSC which is SC and MRC.

This paper shown that GSC $(L_c \neq L)$ achieves the same diversity order as MRC for conventional M-QAM due to the diversity analysis. However the SER performance of GSC is worse than MRC [9]. There is in fact an SNR gap between GSC and MRC even in conventional M-QAM. The SNR gap between SC and MRC in Nakagami-m fading channels has been investigated in [9]. However, it has not commented on the SNR gap between SC and MRC for M-QAM with SSD. In this section the same approach proposed in [9] will be used to investigate the SNR gap for M-QAM with SSD.

B.4.1. Alamouti coded M-QAM with single rotated SSD and GSC SER performance

This subsection compares the theoretical expression derived in Equ. (B.17) to simulated performance of Alamouti coded 4/16/64-QAM with single rotated SSD and GSC for different values of L_c when $L = 3$.

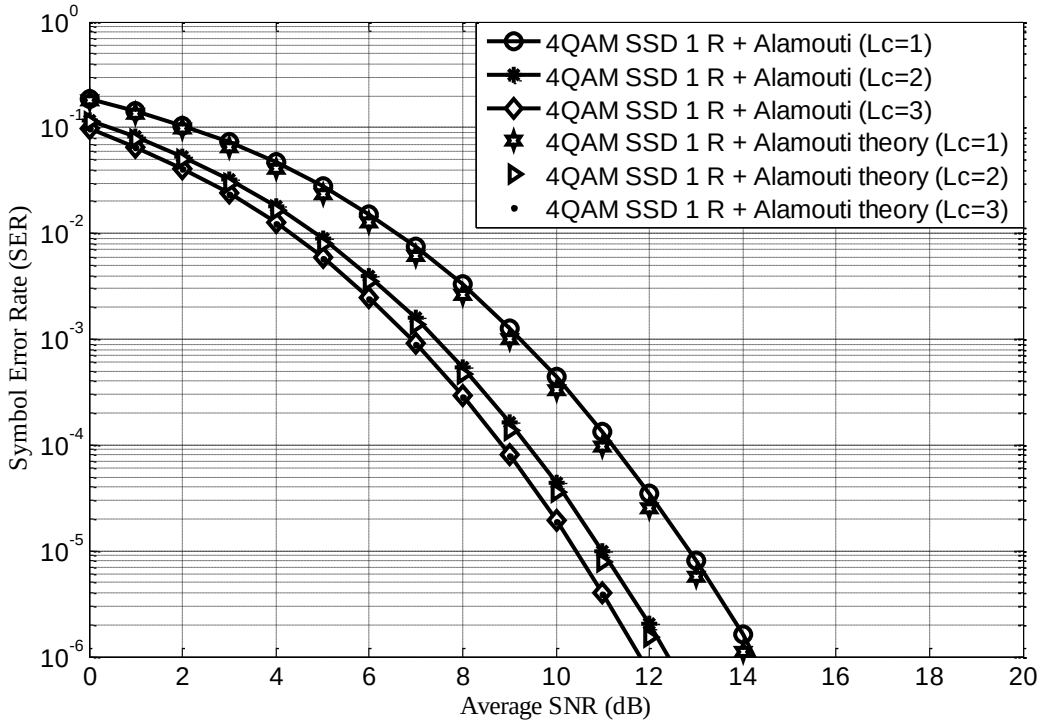

Fig. B. 4: SER of Alamouti coded 4-QAM with 1 rotation SSD and GSC - simulations vs. theory.

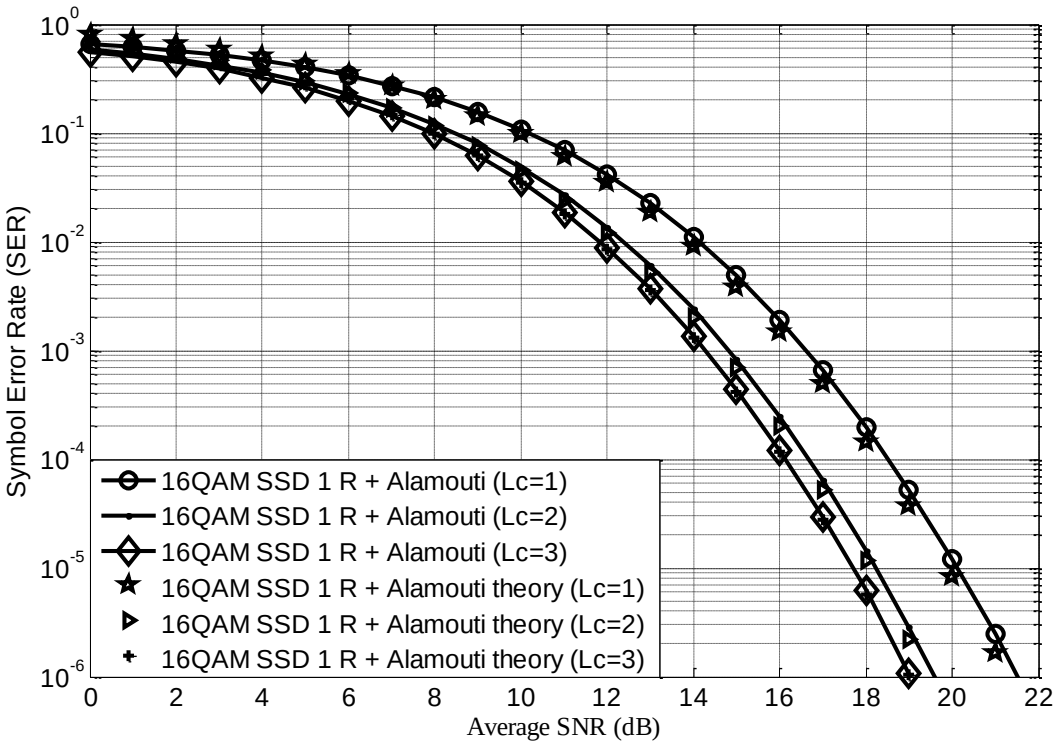

Fig. B. 5: SER of Alamouti coded 16-QAM with 1 rotation SSD and GSC - simulations vs. theory

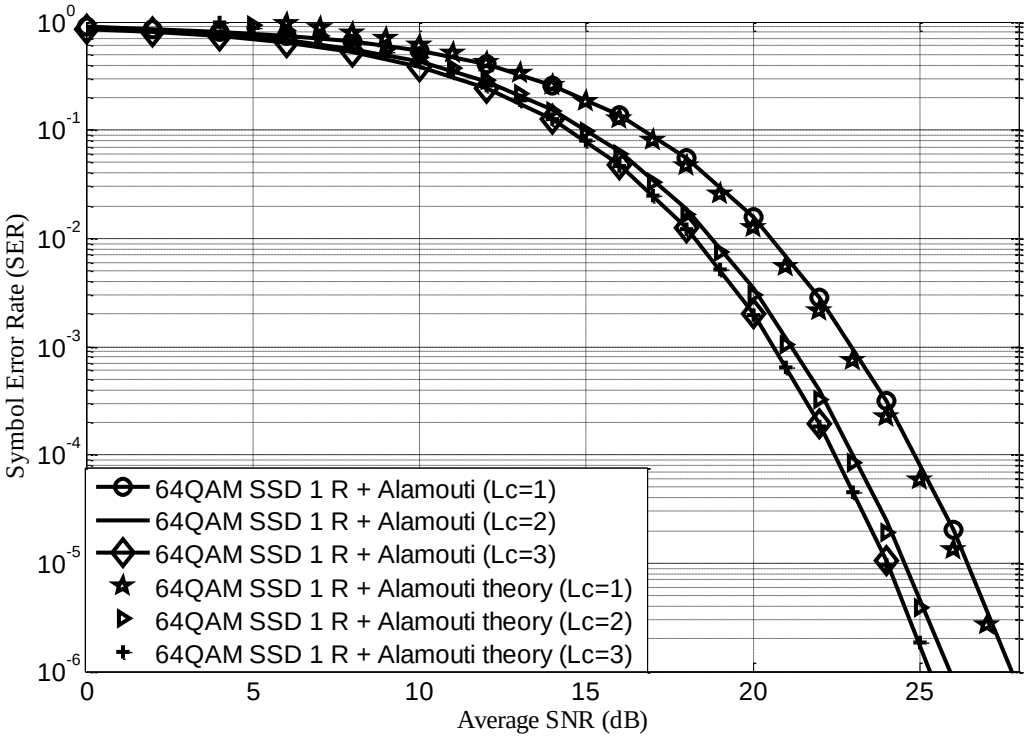

Fig. B. 6: SER of Alamouti coded 64-QAM with 1 rotation SSD and GSC - simulations vs. theory

The simulated performance of Alamouti coded M-QAM with single rotated SSD (denoted by $1R$) and GSC closely match the theoretical expression derived in Equ. (B.17). These results can be viewed in Fig. B 4 to Fig. B 6 for 4, 16 and 64-QAM, respectively. It is observed that an error in simulated vs.

theoretical performance exists, for all M-QAM simulations when $L_c = 1$. It is also observed as more receive antennas are combined for $L_c \geq 2$, this error between theory and simulated performance reduces significantly. The worst case error in predicted performance compared to actual performance amounts to a mere 0.2 dB at a SER of 10^{-6} when $L_c = 1$. At high SNR values such as 20 dB, the error in predicted performance vs. actual performance translates to an error of approximately 1%, therefore becoming negligible. This verifies that the theoretical SER expression derived in Equ. (B.17) is extremely accurate in predicting the performance of Alamouti coded M-QAM with SSD and GSC.

B.4.2. Alamouti coded 4-QAM with 0, 1 and 2 rotation SSD using GSC with a constant number of receive antennas

This subsection will present the SER simulated performance for Alamouti coded 4-QAM with double/single and no rotated SSD with GSC reception. These results are compared to each other when the number of receive antennas remain constant with $L = 3$, but with different GSC cases (different values of L_c).

The diversity order of M-QAM with SSD and GSC is constellation size independent [19] as illustrated by the constant SNR gap between $GSC\ (1,3)$ and $GSC\ (2,3)$ at a SER of 10^{-6} in Fig. B 4 to Fig. B 6 for different M-QAM. Therefore only 4-QAM will be used to show SER performance improvements of Alamouti coded M-QAM with double rotated SSD and GSC.

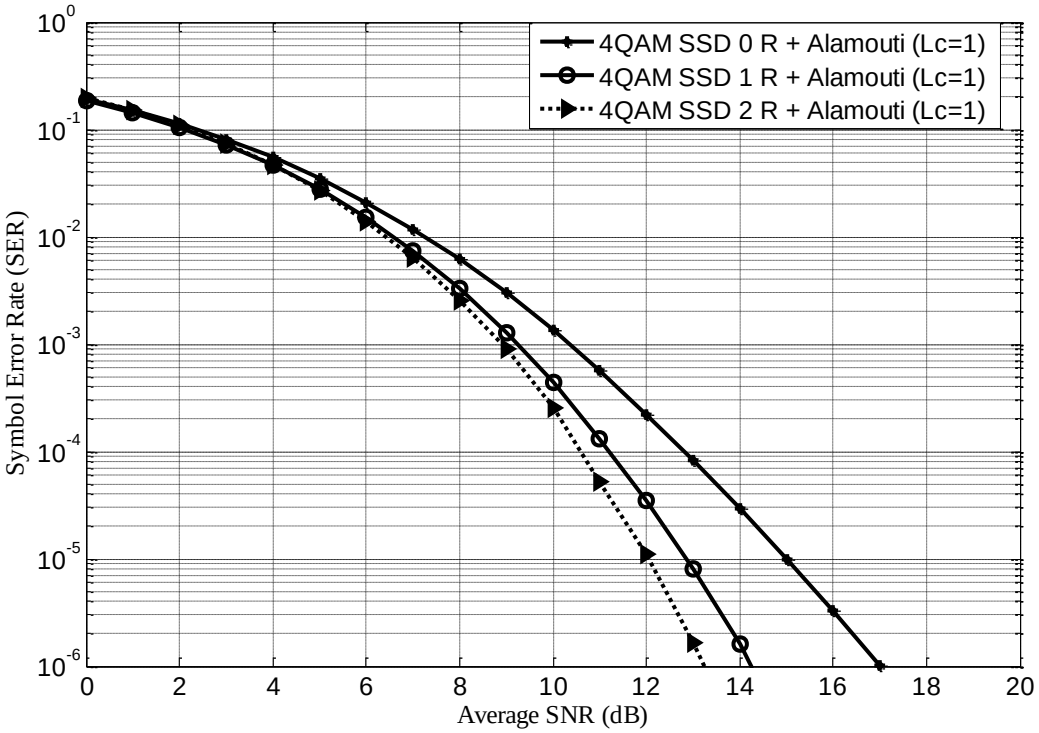

Fig. B. 7: 4-QAM- SER of Alamouti coded 0,1 and 2 rotation SSD and GSC (1,3).

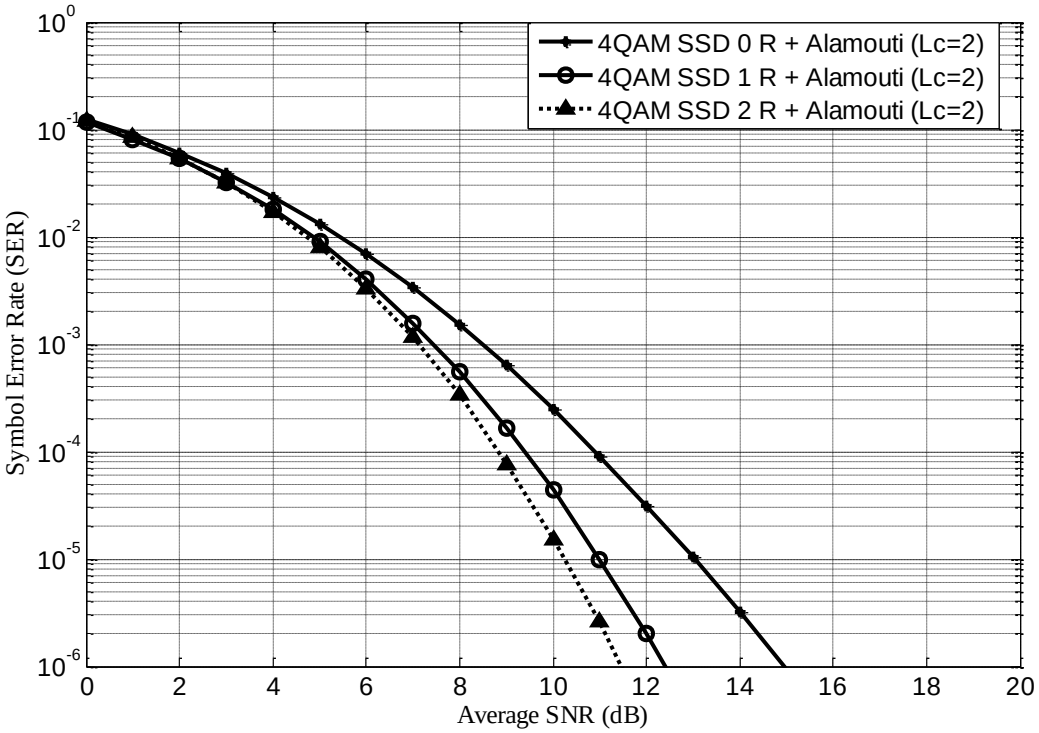

Fig. B. 8: 4-QAM- SER of Alamouti coded 0,1 and 2 rotation SSD and GSC (2,3).

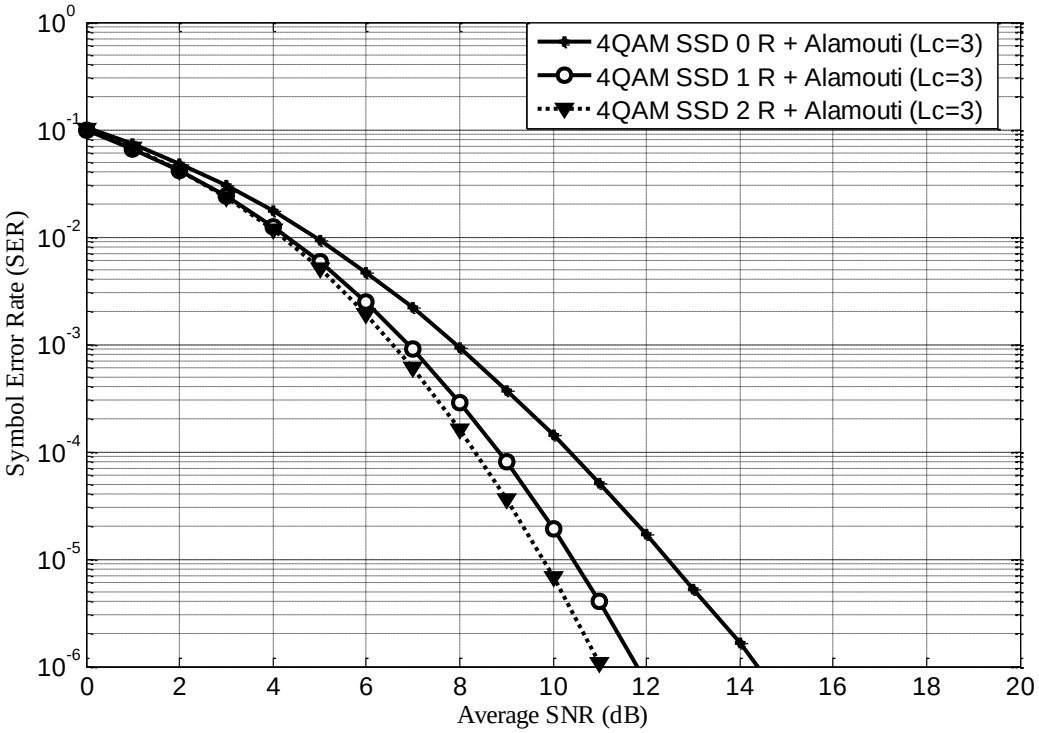

Fig. B. 9: 4-QAM- SER of Alamouti coded 0,1 and 2 rotation SSD and GSC (3,3).

It is observed in Fig. B 7 to Fig. B 9 that Alamouti coded 4-QAM with single rotated SSD and GSC offers better SER performance when compared to Alamouti coded M-QAM with GSC only. Similarly Alamouti coded 4-QAM with double rotated SSD and GSC outperforms Alamouti coded M-QAM with single rotated SSD and GSC. As illustrated by the trend of Fig. B 7 to Fig. B 9, the first rotation results in a larger performance improvement of approximately 2.6 dB whilst a second rotation adds approximately 1 dB, following the same trend and speculating a third rotation will provide less than 1 dB performance enhancement and therefore will not be feasible for such a system. However, Alamouti coded M-QAM with double rotated SSD and GSC does offer advances in SER performance which can be realised in this system.

B.4.3. Alamouti coded 4-QAM with 0, 1 and 2 rotation SSD using GSC with a varying number of receive antennas

In section B.4.2 the SER performance is investigated for single SSD, double SSD and different L_c. It can be seen that the SER performance not only depends on receive diversity, but also depends on signal diversity. This subsection investigates how to choose signal diversity and receive diversity if a target SER is required.

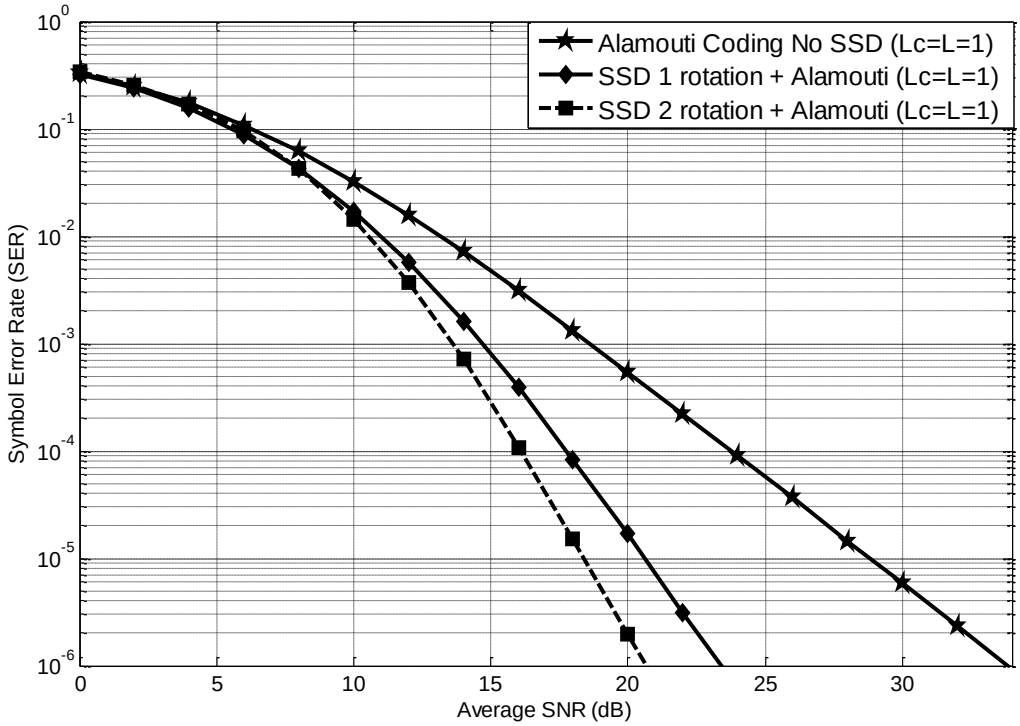

Fig. B. 10: 4-QAM- SER of Alamouti coded 0,1 and 2 rotation SSD and GSC (1,1)

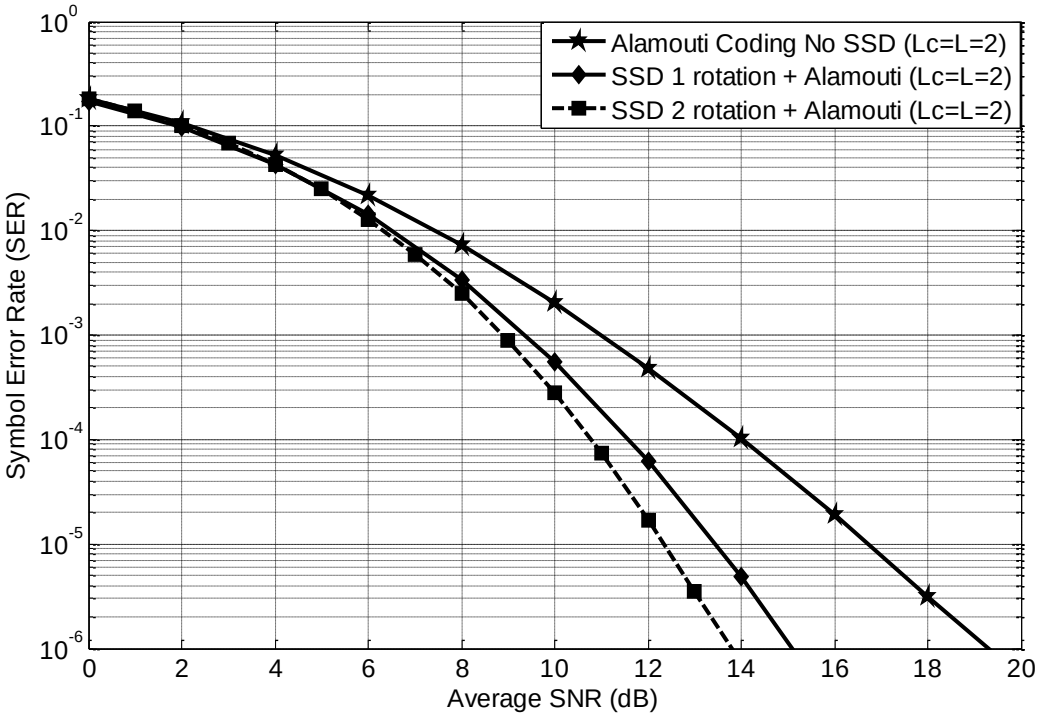

Fig. B. 11: 4-QAM- SER of Alamouti coded 0,1 and 2 rotation SSD and GSC (2,2)

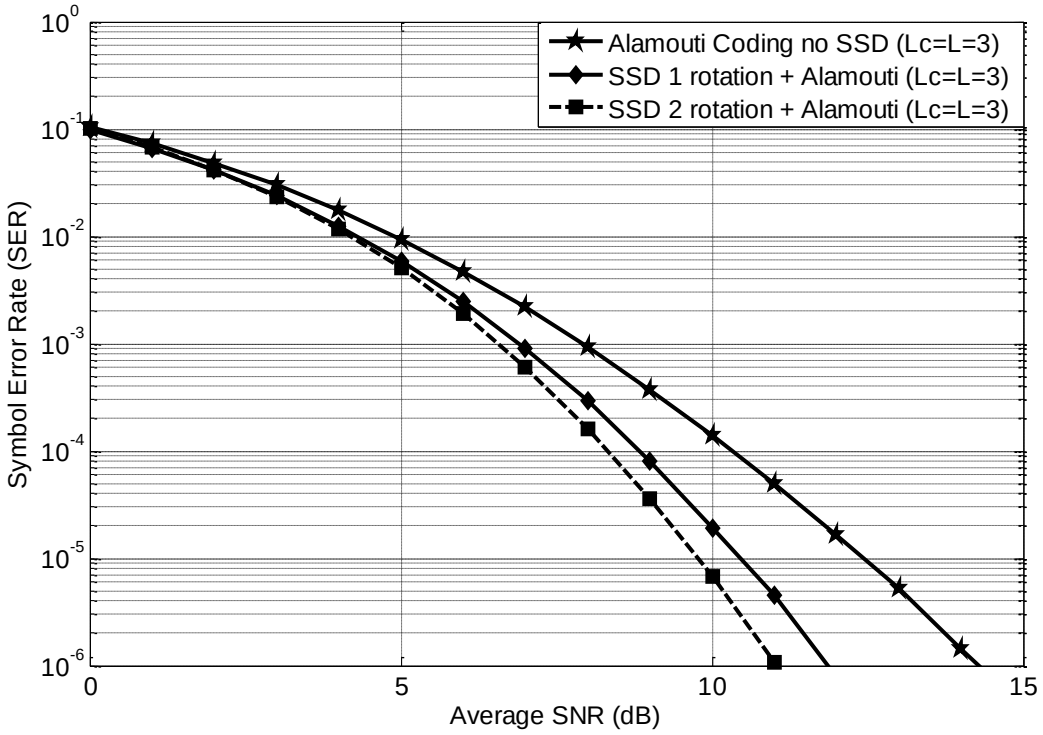

Fig. B. 12: 4-QAM- SER of Alamouti coded 0,1 and 2 rotation SSD and GSC (3,3)

Fig. B. 10 shows that the addition of single and double rotated SSD to an Alamouti coded scheme when $L_c = L = 1$, results in an improvement of approximately 10 dB and 12 dB respectively. Whilst in Fig. B 12 when $L_c = L = 3$, the performance improvement amounts to approximately 2.5 dB and 3.5 dB respectively.

A key observation is the SER performance of Alamouti coded 4-QAM with double rotated SSD with $L_c = L = 2$, provides the same performance as Alamouti coded 4-QAM with $L_c = L = 3$ from Fig. B 11 and Fig. B 9 respectively. The use of Alamouti coded M-QAM with double rotated SSD provides the same level of diversity as adding an extra receive antenna to an Alamouti coded M-QAM with single rotated SSD. The addition of a double rotated constellation to an Alamouti coded M-QAM with SSD and GSC system does increase the detection complexity due to the joint ML detector being applied, however it can result in similar performances as it's single rotated SSD counterpart with an extra receive antenna. This means that detection complexity can be increased in order to decrease physical hardware requirements such as receiver antennas in order to achieve a desired SER performance. In mobile applications this particular result is important as for mobile devices size, weight and cost are always minimised. To conclude when less than three receive antennas are used at the receiver, the use of double rotated SSD will provide a reasonable SNR performance improvement. As the receive antennas are increased this performance improvement decreases substantially. The use of a double rotated constellation can be used as means to provide further diversity to an Alamouti

coded M-QAM with SSD and GSC system at the cost of added complexity but at the reduction of physical antenna requirements.

B.4.4. Alamouti coded 4-QAM with 0, 1 and 2 rotation SSD using SC and MRC with *L*=3 receive antennas.

This section presents the simulation results for 4-QAM SSD with single and double rotation using SC and MRC reception. The purpose of this figure is to show the performance differences between the two extreme cases for single and double rotated SSD.

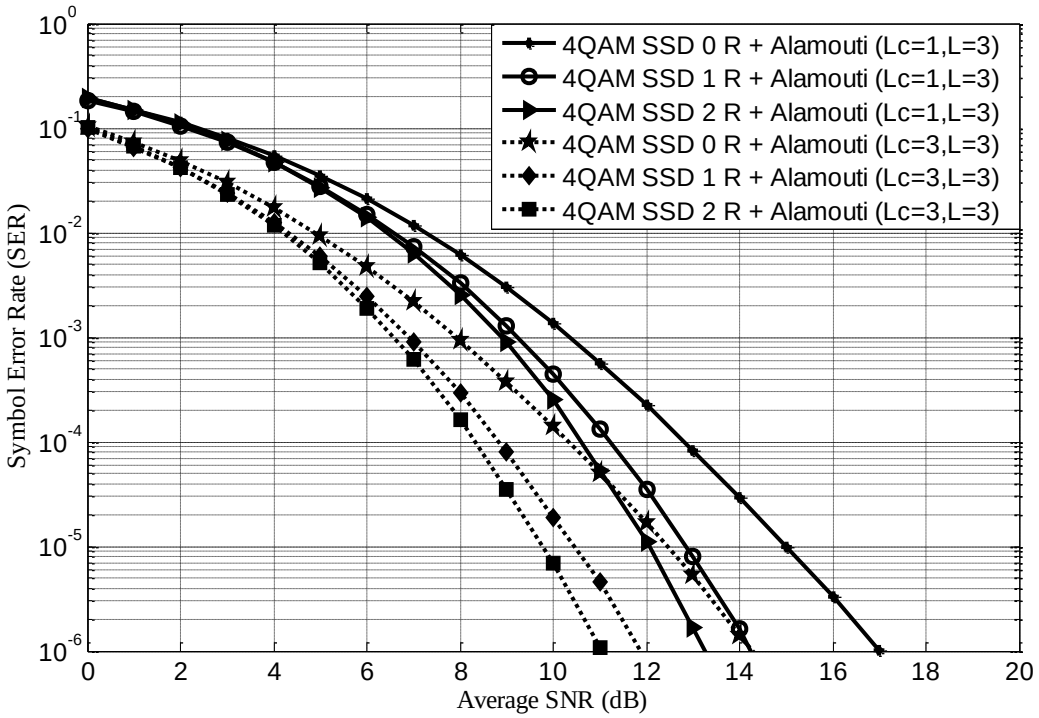

Fig. B. 13: 4-QAM- SER of Alamouti coded 0,1 and 2 rotation SSD with SC and MRC

As expected the MRC case provides better SER performance compared to that of SC for both single and double rotated SSD. However the actual SNR dB performance improvements which are realised when implementing a second rotation is the same increase for both the SC and MRC as can be seen in Fig. B.13, this is largely due to the total receive antennas remaining the same.

B.5. Conclusion

The use of Alamouti transmit antenna diversity with GSC receiver diversity was applied on a rotated constellation as a method to improve the SER. The SER performance of this system was derived for L receive antennas in Rayleigh fading channels based on the NN approach. An MGF function was used to approximate a closed form solution for the SER of Alamouti coded M-QAM with single rotated SSD and GSC. The overall performance of this multiple diversity system outperforms single diversity systems. The simulation results closely matched the closed form theoretical expression found in Equ. (B.17). Alamouti coded M-QAM with double rotated SSD and GSC simulations proved to outperform its single rotated equivalent system. Double rotated SSD can be used as means to introduce additional diversity without the addition of physical antennas but at the cost of additional computational complexity due to the joint ML detector.

The use of GSC with MIMO systems proved to be successful, especially when combined with SSD.. Alamouti coded M-QAM with SSD and GSC has many applications and can be applied to easily introduce diversity into a communication system.

B.6. Appendix

B.6.1 Appendix B1

Based on Fig. B 2, the rotation matrix (B.1) and the original constellation's points results in the following:

$$X_A = \left[3a(\cos\theta) + 3a(-\sin\theta) + i\left(3a\,(\sin\theta) + 3a(\cos\theta)\right)\right] \quad \text{(B.26.1)}$$

$$X_B = \left[a(\cos\theta) + 3a(-\sin\theta) + i\left(a\,(\sin\theta) + 3a(\cos\theta)\right)\right] \quad \text{(B.26.2)}$$

Using equation (B.26.1) and (B.26.2), the Euclidean distances can be computed as follows:

$$d^2_{A\to B} = 4a^2h_I^2\cos^2\theta + 4a^2h_Q^2\sin^2\theta \quad \text{(B.27.1)}$$

$$d^2_{A\to C} = 4a^2h_I^2\,(1 - sin2\theta) + 4a^2h_Q^2(1 + sin2\theta) \quad \text{(B.27.2)}$$

Given h_I and h_Q the conditional PEP of choosing X_B given that X_A was transmitted is given by [15, 19].

$$P\left[X_A \to X_B\,|h_I,\, h_Q\right]_{AL} = \mathrm{Q}\left(\sqrt{\frac{d^2_{A\to B}}{2N_0}}\right) \quad \text{(B.28)}$$

where $Q(\cdot)$ is the Gaussian Q function, h_I and h_Q are the channel gains and $d^2_{A\to B}$ is the Euclidean distance between points X_A and X_B. N_0 is the noise variance given by σ^2.

Using Equ. (B.27.1) and simplifying Equ. (B.28) results in

$$P\left[X_A \to X_B\,|h_I,\, h_Q\right]_{AL} = \mathrm{Q}\left(\sqrt{\left(\frac{2a^2}{N_0}\right)\left(h_I^2\cos^2\theta + h_Q^2\sin^2\theta\right)}\right) \quad \text{(B.29)}$$

Defining the SNR $= \frac{10a^2}{N_0}$ leads to

$$P\left[X_A \to X_B\,|\gamma_I\,,\gamma_Q\,\right]_{AL} = Q\left(\sqrt{\frac{1}{5}SNR\left(h_I^2\cos^2\theta + h_Q^2\cos^2\theta\right)}\right) \quad \text{(B.30)}$$

Equ. (B.30) can be rewritten as

$$P\left[X_A \to X_B\,|\gamma_I\,,\gamma_Q\,\right]_{AL} = \qquad Q\left(\sqrt{\frac{1}{5}\left(\gamma_{\mathrm{I}}\cos^2\theta + \gamma_{\mathrm{Q}}\cos^2\theta\right)}\right) \quad \text{(B.13.1)}$$

where $\gamma_I = SNR(h_I)^2$ and $\gamma_Q = SNR\left(h_Q\right)^2$.

Similarly we have

$$P\left[X_A \rightarrow X_C \,|\gamma_I\,,\gamma_Q\,\right]_{AL} = Q\left(\sqrt{\frac{1}{5}\left(\gamma_{\mathrm{I}}\ (1+\sin 2\theta)\ +\gamma_{\mathrm{Q}}\ (1-\sin 2\theta)\ \right)}\right) \qquad \text{(B.13.2)}$$

B.6.2 Appendix B2

A closed form SER will be evaluated using an MGF function. An MGF is defined as follows [4]

$$M_y\,(s) = \int_0^{\infty} f_{\gamma}(\gamma)\ e^{s\gamma}\,\mathrm{d}\gamma \qquad \text{(B.29)}$$

A trapezoidal approximation for the Q function found in [6] presented below.

$$Q(x) = \frac{1}{2n}\left(\frac{1}{2}e^{-\frac{x^2}{2}} + \sum_{k=1}^{n-1} e^{-\frac{x^2}{2\sin^2\theta_k}}\right) \qquad \text{(B.30)}$$

where $\theta_k = \frac{k\pi}{2n}$ and n is the upper limit of the summation.

Substituting Equ. (B.30) into Equ. (B.13.1) and using this result into Equ. (B.14) results in the following:

$$P[X_A \rightarrow X_B\,]_{AL} = \int_0^{\infty}\int_0^{\infty}\left\{\frac{\Delta_1}{4n} + \left(\frac{1}{2n}\sum_{k=1}^{n-1}\Delta_2\right)\right\}\ f_{\gamma_I}(\gamma_I) f_{\gamma_Q}(\gamma_Q)\mathrm{d}\gamma_I\mathrm{d}\gamma_Q \qquad \text{(B.31)}$$

where $f(\gamma_I)$ and $f(\gamma_Q)$ is given by Equ. (B.10), $\Delta_1 = e^{-\frac{\frac{1}{5}\left(\gamma_I\ \cos^2\theta+\gamma_Q\ \sin^2\theta\right)}{2}}$ and $\Delta_2 = e^{-\frac{\frac{1}{5}\left(\gamma_I\ \cos^2\theta+\gamma_Q\ \sin^2\theta\right)}{2\sin^2\theta_k}}$.

Simplifying the expression in Equ. (B.31) with Equ. (B.29) results in Equ. (B.15)

$$\begin{aligned} P[X_A \rightarrow X_B\,]_{AL} = {} & \frac{1}{4n} M_{\gamma GSC_{AL}}\left(-\frac{\Omega_1}{10}\right) M_{\gamma GSC_{AL}}\left(-\frac{\Omega_2}{10}\right)\ + \\ & \frac{1}{2n}\sum_{k=1}^{n-1} M_{\gamma GSC_{AL}}\left(-\frac{\Omega_1}{10\sin^2(\theta_k)}\right) M_{\gamma GSC_{AL}}\left(-\frac{\Omega_2}{10\sin^2(\theta_k)}\right) \end{aligned} \qquad \text{(B.15)}$$

where $\Omega_1 = \cos^2\theta$, $\Omega_2 = \sin^2\theta$, $\Omega_3 = (1+\sin 2\,\theta)$, $\Omega_4 = (1-\sin 2\,\theta)$ and $M_{\gamma GSC_{AL}}$ given by Equ. (B.11).

B.7. References

[1] H. Xu, "Symbol Error Probability for Generalized Selection Combining," *SAIEE Research Journal*, vol. 100, no. 3, pp. 68-71, Sept 2009.

[2] A. Malaga and A. Parl Steen, "Experimental Comparison of Angle and Space Diversity for Line-of-Sight Microwave Links," in *MILCOM. IEEE VOL2*, Boston, USA, 1985, pp. 382-386.

[3] K. K. Wong, "Performance Analysis of Single and Multiuser MIMO Diversity Channels Using Nakagami- m Distribution," *IEEE Trans. on Wireless communications*, vol. 3, no. 4, pp. 1043-1047, July 2004.

[4] M. S Alouini and M. K. Simon, *Digital Communications over Fading Channels: A Unified Approach to Performance Analysis*.: A Wiley- Interscience Publication, 2000.

[5] S. Alamouti, "A simple transmit diversity technique for wireless communications," *IEEE, Selected areas on Comm.*, vol. 16, no. 8, pp. 1451-1458, Oct 1998.

[6] A. Saeed, H. Xu, and T. Quazi, "Alamouti space-time block coded hierarchical modulation with signal sapce diversity and MRC reception in Nakagami-m fading channels.," *IET communications*, vol. 8, no. 4, pp. 516-524, Oct 2014.

[7] J. Boutros and E. Vitebro, "Signal Space Diversity: A Power-and Bandwidth- Efficient Diversity Technique," *IEEE Trans. on Info. theory*, vol. 44, no. 4, pp. 1453 - 1467, July 1998.

[8] J Kim and I. Lee, "Analysis of Symbol Error Rates for Signal Space," in *IEEE Int Conf. on communications*, Beijing, 2008, pp. 4621 - 4625.

[9] S. Jeon, J. Lee, I. Kyung, and M.k. Kim, "Component Interleaved Alamouti Coding with Rotated Constellations for Signal Space Diversity.," in *IEEE International (BMSB)*, Shanghai, 2010, pp. 1-6.

[10] Z. Paruk and H. Xu, "Performance Analysis and Simplified Detection for Two - Dimensional Signal Space Diversity," *SAIEE Africa Research Journal*, vol. 104, no. 3, pp. 97-106, September 2013.

[11] J. Kim, H. Kim, T. Jung, J. Bae, and L. Gwangsoon, "New Constellation- Rotation Diversity Scheme for DVB-NGH," in *VTC IEEE*, Ottawa, 2010, pp. 1-4.

[12] Z. Paruk and H. Xu, "Performance Analysis and Simplified Detection for Two - Dimensional Signal Space Diversity with MRC reception," *SAIEE Africa Research Journal*, vol. 104, no. 3, pp. 97-106, September 2013.

[13] S.A. Ahmadzadeh, "Signal space cooperative communication," *IEEE Trans. on wirless*

communications., vol. 6, no. 4, pp. 1266-1271, April 2010.

[14] G. Taricco and E. Viterbo, "Performance of component interleaved signal sets for fading channels," *Electronic letters*, vol. 32, no. 13, pp. 1170-1172, April 1996.

[15] S. Jeon, I. Kyung, and M.K. Kim, "Component- Interleaved receive MRC with Rotated Constellation for Signal Space Diversity.," in *IEEE Conf. Vehicular Technology*, Alaska, 2009, pp. 1-6.

[16] K. N. Pappi, N. D. Chatzidiamantis, and G. K. Karagiannidis, "Error Performance of Multidimensional Lattice Constellations—Part I: A Parallelotope Geometry Based Approach for the AWGN Channel," *IEEE trans. on communications.*, vol. 61, no. 3, pp. 1088-1098, April 2013.

[17] K.N. Pappi, "Error Performance of Multidimensional Lattice Constellations—Part II: Evaluation over Fading Channels," *IEEE Trans. on communcations*, vol. 61, no. 3, pp. 1099-1110, April 2013.

[18] M.S. Alouini and M.K. Simon, "An MGF -Based Performance Analysis of Generalized Selection Combining over Rayleigh Fading Channels," *IEEE Trans. on communications*, vol. 48, no. 3, pp. 401-415, March 2000.

[19] M. Salehi and J. G. Proakis, *Digital Communications*, 5th ed. San Diago, USA: McGraw - Hill Higher Education, 2007.

[20] K. Xu, "Antennas Selection for MIMO Systems over Rayleigh Fading Channels.," in *ICCCAS*, Chengdu, 2004, pp. 185-189.

[21] A. Essop and H. Xu, "Symbol Error Rate of Generalized Selection Combining with Signal Space Diversity in Rayleigh Fading Channels," July 2014.

Part III

Conclusion

Conclusion

Performance of wireless communications is enhanced via individual diversity techniques and further improvements can be realised by exploiting the benefits of combining multiple diversity techniques. SSD with spatial diversity provides a substantial level of diversity making it more resilient to multipath fading and improving SER performance. The content of this dissertation presents communication schemes which improve the SER. Paper A, introduced M-QAM with SSD and GSC at an optimum rotation angle whilst paper B expanded this approach to incorporate Alamouti coding scheme.

In paper A, an M-QAM system with SSD and GSC in Rayleigh fading was investigated. A closed form solution was presented and this was successfully validated via simulations. Rotation angles for SSD were researched and two previously discussed methods to derive an optimal angle were compared to each other with aid of simulations. An optimum angle derived by maximising the minimum product distance resulted in optimal performance. A diversity analysis revealed that the extreme cases of GSC when L_c= 1 and $L_c = L$, both provide the same level of diversity as the SNR tends to infinity however there exists a small SNR gap between different GSC (different L_c values). It was proved that although MRC is the best performing, the dB in SER performance gained between each L_c step from SC to MRC, becomes increasingly smaller, therefore validating the use of GSC. This phenomena was further researched with the presentation of the SNR gap between different L_c cases when L remains constant. The results revealed a mere 0.2 dB gain between switching from GSC(4,5) to GSC(5,5) (MRC with $L_c = L = 5$), questioning the application of the most complex MRC and increasing motivation for the use of less complex high performing GSC.

Paper B, is an extension of paper A and includes an additional diversity compared to the system of paper A. Alamouti coded M-QAM was applied to the system presented in paper A. The closed form theoretical expression closely matched the simulated performance of the system, validating the performance of Alamouti coded M-QAM with SSD with GSC for single rotation. Alamouti coded M-QAM with double rotated SSD and GSC was also investigated. Simulation results revealed a substantial gain in performance when applying two rotations. It was found that an Alamouti coded M-QAM with double rotated SSD and GSC ($L_c = 2, L = 2$) performed the same or better than an Alamouti coded M-QAM with single rotated SSD with GSC ($L_c = 3, L = 3$), providing an additional level of diversity without the addition of more receive antennas but at the addition of detection complexity.

In conclusion the work presented in this dissertation provides insight into new approaches to improve wireless communications reliability in terms of SER performance and the aim to enhance wireless communications was successfully fulfilled.